Rho-dependent transcriptional switches regulate the bacterial response to cold shock

Mildred Delaleau, Nara Figueroa-Bossi, Thuy Duong Do, Patricia Kerboriou, Eric Eveno, Lionello Bossi, Marc Boudvillain

Rho-dependent transcriptional switches regulate the bacterial response to cold shock

Mildred Delaleau[1], Nara Figueroa-Bossi[2], Thuy Duong Do[1,3], Patricia Kerboriou[2], Eric Eveno[1], Lionello Bossi[2], and Marc Boudvillain[1,3,4]

[1]Centre de Biophysique Moléculaire, CNRS UPR4301, affiliated with Université d'Orléans, rue Charles Sadron, 45071 Orléans cedex 2, France.

[2]Université Paris-Saclay, CEA, CNRS, Institut de Biologie Intégrative de la Cellule (I2BC), 91190 Gif-sur-Yvette, France.

[3]ED 549, Sciences Biologiques & Chimie du Vivant, Université d'Orléans, France.

[4]Corresponding author (marc.boudvillain@cnrs.fr)

Running title: Cold-shock Rho-dependent riboswitches

ABSTRACT

Rho-dependent transcription termination plays a pivotal role in the regulation of bacterial gene expression. Binding of the Rho helicase to the nascent transcript triggers termination in response to cellular signals that directly or indirectly modulate mRNA structure and the accessibility of Rho utilization (*Rut*) sites. Despite the impact of temperature on RNA structure, Rho-dependent termination has never been associated to the bacterial response to temperature shifts. Here, we show that Rho is in fact a central player in the cold shock response (CSR), challenging the conventional view that CSR is primarily a posttranscriptional program. We identify *Rut* sites in the 5' untranslated regions of key CSR genes/operons (*cspA*, *cspB*, *cspG*, *nsrR-rnr-yjfHI*) that trigger premature termination by Rho at 37°C but not at 15°C, *in vitro* and *in vivo*. High concentration of the RNA chaperone CspA or base-pair mutations in the *cspA* mRNA leader can shift the balance between termination and antitermination, revealing how Rho can be controlled through RNA restructuring to activate CSR genes during the cold shock, and then to silence these genes during cold acclimation. Overall, the work presented here sets a new paradigm for how RNA thermosensors can modulate gene expression.

INTRODUCTION

The cold shock response (CSR) is a complex and highly orchestrated set of molecular events that enables bacteria to cope with sudden temperature downshifts and to maintain cellular homeostasis under low temperature conditions. In *Escherichia coli* and various other mesophilic bacteria, an abrupt decrease in temperature causes the arrest of cell growth and a drastic reduction of mRNA translation due, among others, to increased structuring of the mRNAs. The CSR proteins escape this general inhibition and are involved in a variety of cold acclimation processes such as the remodeling of cell membrane composition or the facilitation of nucleic acid transactions thermodynamically constrained by the lower temperature. Some CSR proteins are upregulated transiently during cold acclimation while others are produced at high levels for as long as cold persists. Cold acclimation can take several hours during which bulk protein synthesis gradually increases until cells are sufficiently cold-adapted to resume growth, albeit at a slower rate (reviewed in ref. [1-3]).

In *E. coli*, two CSR proteins appear to play a central role in cold acclimation by dynamically regulating gene expression at the posttranscriptional level. The RNA chaperone CspA helps unfold mRNA structures that are formed at low temperatures and impede translation while the [3'→5'] exoribonuclease RNase R, which is not inhibited by RNA secondary structures, stimulates the degradation and turnover of mRNAs.[4] The expression of RNase R (encoded by *rnr*) is induced 8-15 fold upon cold shock, an increase attributed to cold-induced folding and increased mRNA stability against degradation.[5,6] The expression of CspA is also stimulated following a cold shock (by a factor that varies with growth stage), in part through greater protection of the *cspA* mRNA against ribonucleases[7,8], but also largely through the regulation of *cspA* translation.[4,9,10] Indeed, contrary to most RNAs in the cell, the *cspA* mRNA folds into a structure favoring efficient translation at low temperatures (e.g. 15°C) whereas, at 37°C, the mRNA adopts a conformation inhibiting translation.[4,9] Notably, binding of CspA to the "15°C-conformation" can trigger an mRNA rearrangement less favorable to translation[4] thereby providing a negative feedback control on CspA expression during the CSR.[11] Conversely, Binding of CspA to the "37°C conformation" stimulates *cspA* translation.[12] This may contribute to the basal expression and abundance of CspA during early exponential growth at 37°C.[13,14] Sequence elements critical for the posttranscriptional regulation of *cspA*

have been identified in its 5' untranslated region (5'UTR) and in the initial section of its coding sequence (CDS).[4,9,10,12,15,16]

There are nine Csp (cold shock protein) homologues in *E. coli* but only expression of CspA, CspB, CspG, and CspI is induced by cold shock (**Supplementary Figure 1**).[1-3] Although some of these proteins share regulatory features and have partially redundant functions[4,17-19], CspA stands out as the primary contributor to the CSR due to its remarkable abundance. Upon cold shock, CspA production can indeed represent close to 15% of total protein synthesis.[11,20] Thus, despite a modest affinity for RNA (K_d in µM range)[12,21], the high concentration of CspA in cold-shocked cells (~100 µM)[22] and its fairly relaxed sequence specificity[2] enables its widespread binding to and unfolding of cellular RNA. This process largely contributes to the reduction of global mRNA structure and to the recovery of bulk translation during the cold acclimation phase.[4]

While the regulatory interplay between mRNA structure, translation, and decay during cold acclimation is relatively well established[1-3], the contribution of transcription, in particular its elongation phase, remains uncertain despite early work suggesting its potential significance. In one instance, incremental deletions of the long 5'UTR of *cspA* were shown to strongly stimulate the production of the mRNA independently of cold shock.[23] Since the deletions did not change the rate of decay of the *cspA* mRNA, the authors postulated that the 5'UTR might be "involved in negative regulation of the cspA gene expression at the level of transcription". Transcription initiation is not the regulated step[7] but CspA binding to the 5'-leader of its own mRNA stimulates transcriptional pausing in the 5'UTR, which could play a role.[24] However, CspA inhibits other pause signals or intrinsic transcription terminators, most likely by preventing the formation of the corresponding RNA hairpin structures[25], and is thus usually regarded as a positive rather than negative transcription regulator.[1-3]

A source of negative transcriptional regulation in bacteria is Rho-dependent termination (**Figure 1**), which silences hundreds of genomic loci in *E. coli*[26-28] and has been implicated in several conditional attenuation mechanisms (reviewed in ref. [29-31]). However, to our knowledge, the involvement of Rho-dependent termination in the CSR has not been investigated. This is somewhat surprising given that cold shock is expected to produce widespread decoupling of translation from transcription[32,33] and that Rho-dependent termination is the main mechanism of surveillance of transcription-translation coupling

(**Figure 1**, bottom; reviewed in ref. [34,35]). In addition, increased mRNA structuring at low temperature may hide *Rho utilization* (*Rut*) sites and inhibit termination by preventing Rho access to the transcript (**Figure 1**, top right) in a manner reminiscent of the riboswitch-like mechanisms used by some Rho-dependent transcriptional attenuators.[36,37]

Here, we present comprehensive evidence for the involvement of Rho in the cold shock response. We identify *Rut* sites in the 5'UTRs of genes or operons involved in the CSR (*cspA*, *cspB*, and *cspG* genes and *nsrR-rnr-yjfHI* operon) and show that transcription of these genes/operons is prematurely terminated by Rho at 37°C but not at 15°C*, in vitro* and *in vivo*. We also demonstrate that CspA can restore Rho-dependent termination at 15°C, implying that dual-input, antagonistic control (T° vs Csp concentration) of transcriptional attenuation contributes to the dynamic regulation of cold shock genes during the acclimation phase. Altogether, our results unveil the existence of an upper layer of regulation in the bacterial response to cold stress and a novel mechanism through which RNA thermosensors modulate gene expression.

RESULTS AND DISCUSSION

Identification of Rut sites in the 5'UTRs of cold shock genes

In a previous study, we mapped putative *Rut* sites along the genome of *E. coli* using a new global screening approach that we named "Helicase-SELEX".[38] Close examination of the Helicase-SELEX data revealed that a number of putative *Rut* sites localized within the 5'UTRs of genes involved in the CSR, namely *cspA*, *cspB*, *cspG*, *lpxP* (encoding a palmitoleoyl-transferase involved in cold adaptation of the membrane), and *nsrR* (at the start of the *nsrR-rnr-yjfHI* operon) as well as in the initial section of the *rnr* CDS (**Figure 2A**). Interestingly, these putative *Rut* sites matched some of the so-called bicyclomycin-sensitive regions previously detected in genome-wide analyses of the transcriptional response to Rho inhibitor bicyclomycin (see supporting data in ref. [26,27] and **Figure 2A**). These regions were not discussed specifically in these previous studies and have remained overlooked until now.

To substantiate the presence of Rho-dependent terminators in these regions of the *E. coli* genome, we first calculated the percentages of C and G residues along the coding DNA strand, in search of large C>G biases (aka C>G bubbles) characteristic of Rho-dependent

terminators.[39,40] In each case, a C>G bubble overlapping with the putative *Rut* site uncovered by Helicase-SELEX was indeed found (**Figure 2B**). Next, we performed *in vitro* transcription experiments with DNA templates encoding the upstream sections of the relevant transcription units (5'UTR and first ~200-400 nucleotides [nt] of the CDS) under control of the strong T7A1 promoter.[40] We also used a DNA template encoding the Rho-dependent λtR1 terminator as positive control.

Rho-dependent termination signals were detected in all instances when the transcription reactions were carried out at 37°C in presence of Rho (**Figure 2**, 'Term'). Addition of transcription factor NusG stimulated the production of Rho-dependent truncated transcripts, including at sites closer to the promoter, as observed under similar conditions for other Rho-dependent terminators (e.g. in ref. [37,41-43]). Importantly, the termination regions detected *in vitro* (**Figure 3A-E**) are located immediately downstream from the C>G bubbles and putative *Rut* sites (**Figure 2B**), consistent with Rho-dependent termination initiating in the 5'-leader regions of the cold shock genes. A notable exception is *lpxP*, which has a shorter 5'UTR (67 base pairs [bp]) than the other cold shock genes (146-161 bp) and for which the termination region starts ~50 bp downstream from the start codon (**Figure 3E**).

A strong *in vitro* Rho-dependent termination signal was also detected in the CDS of the *rnr* gene, ~100 bp downstream from the short (38 bp) intergenic *nsrR-rnr* region (**Supplementary Figure 2A**). This intragenic signal complements the upstream termination signal located in the 5'UTR of the *nsrR-rnr-yjfHI* operon (**Figure 3D**), in good agreement with observations from genome-wide studies (**Figure 2**). Altogether, these data support the presence of Rho-dependent termination signals in the 5'UTRs of *cspA*, *cspB*, *cspG*, and *nsrR* and in the upstream parts of the *lpxP* and *rnr* CDSs.

Temperature governs Rho-dependent transcriptional attenuation of cold shock genes

Results were radically different for some of the DNA templates when the transcription reactions were carried out at 15°C instead of 37°C. Most notably, the formation of Rho-dependent truncated transcripts was strongly inhibited with templates *cspA*, *cspB*, and *cspG* (**Figure 3A-C**, right gels). With template *nsrR*, termination within the 5'UTR was also strongly inhibited at 15°C while a new site of strong Rho-dependent termination became apparent

farther downstream in the *nsrR* CDS (**Figure 3D**, star). By comparison, the Rho-dependent termination profiles obtained with templates *lpxP* (**Figure 3E**), λtR1 (**Figure 3F**), and *rnr* (**Supplementary Figure 2A**) were much less affected by the decrease in reaction temperature. Taken together, these data strongly suggest that the 5'-leaders of the *cspA*, *cspB*, *cspG*, and *nsrR* genes adopt structures at 15°C that prevent Rho-dependent termination, most likely because they hide the *Rut* sites from Rho (**Figure 1**, top right). By contrast, RNA folding at 15°C does not effectively shield the *lpxP*, *rnr*, and λtR1 terminators nor the downstream *nsrR* terminator (*) from Rho action. Thus, temperature may regulate the expression of *cspA*, *cspB*, *cspG,* and *nsrR-rnr-yjfHI* by a conditional Rho-dependent attenuation mechanism. This transcriptional regulation, working alongside the established posttranscriptional mechanisms[4-10], is expected to ensure the tightest form of control in a manner akin to the multilayered *modus operandi* of some riboswitches.[31] Finally, the experiment in Figure 3 shows that CspA, at the sub-saturating concentration of 0.5 µM ($_{low}$[CspA]), has no effect on Rho-dependent transcription termination with the tested DNA templates at both 15°C and 37°C (see more about this point below).

To determine if the above findings hold true *in vivo*, we first compared the amounts of *cspA* transcripts formed in WT (*rho*$^{+}$) and *rho*^{R66S} strains of *E. coli* MG1655. The *rho*^{R66S} mutant is viable but defective in the termination of many transcripts[44,45], presumably because the R66S mutation weakens Rho binding to *Rut* sites.[46] Total RNA was extracted from log phase cultures of the *rho*$^{+}$ and *rho*^{R66S} strains after they were either cold-shocked at 15°C or kept at 37°C for 30 min. To detect the full-length *cspA* mRNA (*cspA*-FL, hereafter) and potentially shorter species, we performed northern blots with a ^{32}P-labeled oligonucleotide probe hybridizing to the +3 to +48 region of the *cspA* 5'leader (+1 being the transcription start site).

Formation of *cspA*-FL was readily detected in the cold-shocked cells, with no significant difference in *cspA*-FL abundance between the *rho*$^{+}$ and *rho*^{R66S} strains (**Figure 4A**; $p = 0.41$, unpaired, two-tailed Student's t-test). Results were dramatically different for cells cultured at 37°C throughout. In this case, *cspA*-FL was weakly expressed in the *rho*^{R66S} strain and almost undetectable in the *rho*$^{+}$ strain (**Figure 4A**). Overall, *cspA*-FL was around two orders of magnitude more abundant in the *rho*^{R66S} mutant than in the *rho*$^{+}$ strain at 37°C but still two orders of magnitude less abundant than in the cold-shocked cells ($p < 0.05$; unpaired, two-tailed Student's t-tests). Moreover, the proportions of truncated *cspA* transcripts were

198 comparatively much lower in the cold-shocked cells (**Figure 4A**, graphs). These dramatic
199 effects cannot be explained by concomitant changes in the cellular levels of Rho or RNA
200 polymerase, which do not vary much upon cold shock (**Supplementary Figure 1**).[4] Rather, they
201 are consistent with the *in vitro* data from above and support the scenario in which Rho-
202 dependent termination downregulates *cspA* in exponentially growing cells at 37°C whereas
203 cold shock triggers anti-termination and thus stimulates *cspA* expression at the co-
204 transcriptional level.

205 Similar Northern Blot experiments were performed with oligonucleotide probes
206 hybridizing to the 5'UTRs of *cspB* and *cspG*. In the case of *cspB*, signals were weaker than for
207 *cspA* but the trend was similar, i.e. full-length *cspB* mRNA was barely detected at 37°C, and
208 only in the *rho*^{R66S} mutant, but was present in considerably higher amounts in both *rho*$^{+}$ and
209 *rho*^{R66S} strains after cold-shock (**Supplementary Figure 3A**). Moreover, the signal for the full-
210 length *cspB* mRNA in the *rho*^{R66S} mutant was more easily detected when cells were cultured
211 at 30°C instead of 37°C, which is consistent with the lower temperature of induction of *cspB*
212 as compared to *cspA*.[47] Similarly, we detected a weak signal for the full-length *cspG* mRNA at
213 30°C, but not at 37°C, in the *rho*^{R66S} mutant only, whereas we observed a strong induction of
214 *cspG* after cold-shock in both *rho*$^{+}$ and *rho*^{R66S} strains (**Supplementary Figure 3B**). Note that in
215 contrast to *cspA* and *cspB*, the optimal temperature of induction for *cspG* has not been
216 determined.

217 To probe the polycistronic *nsrR-rnr-yjfHI* transcript products, we used denaturing 1.5%
218 agarose (instead of 8% polyacrylamide) electrophoresis and two distinct oligonucleotide
219 probes for Northern blotting: probe A hybridizes to the 5'UTR of *nsrR* while probe B hybridizes
220 to the intergenic region between the *nsrR* and *rnr* genes. With both probes, we detected two
221 diffuse bands (**Figure 4B**) reflecting the complex biogenesis and posttranscriptional processing
222 of the *nsrR-rnr-yjfHI* transcripts.[5,6] The intensities of the two bands were higher after cold-
223 shock (**Figure 4B**), confirming the stabilization of the transcripts under this condition.[5,6] The
224 intensities of the bands were also higher in the *rho*^{R66S} mutant than in the *rho*$^{+}$ strain,
225 supporting Rho involvement in the regulation of *nsrR-rnr-yjfHI* expression. The effect of the
226 *rho*^{R66S} mutation was particularly marked for the longest transcript species (slowest migrating
227 band) and was still noticeable for this species at 15°C. These observations support a scenario
228 where Rho-dependent polarity along the *nsrR-rnr-yjfHI* transcription unit is mediated by

several Rho-dependent signals such as those detected *in vitro* in the 5'UTR and in the CDS of *nsrR* and that operate at high and low temperatures, respectively (**Figure 3D**). Of note, translation of the *nsrR gene* is very inefficient[48] and may thus not adequately mask the intragenic termination signal (**Figure 3D**, star) *in vivo*. By contrast, the downstream *rnr* gene is efficiently translated, in particular at low temperature[49], which should mask the Rho-dependent signal in the *rnr* CDS (**Supplementary Figure 2A**).

To confirm our *in vivo* observations, we performed quantitative RT-PCR experiments with pairs of primers hybridizing in the coding regions of *cspA*, *cspB*, cspG, *nsrR*, *rnr*, and *lpxP*. As a control, we first performed RT-PCR quantification of the *rho* gene, which is regulated by Rho-dependent attenuation[50] The RT-qPCR signal for *rho* was indeed higher in the *rho*^{R66S} mutant than in the *rho*$^{+}$ strain and this difference was highly significant at both 37°C and 15°C (**Figure 4C**), suggesting that the Rho-dependent attenuator controlling *rho* expression is not much affected by cold shock. For each strain, the differences in *rho* signals between 37°C and 15°C were modest (less than 5-fold), confirming that *rho* mRNA levels do not vary much upon cold shock.[4] By contrast, we observed dramatic increases of the RT-qPCR signals for *cspA*, *cspB*, and *cspG* upon cold shock and large differences between the signals for the *rho*$^{+}$ and *rho*^{R66S} strains at 37°C (15-40 fold), which however were cancelled out at 15°C (**Figure 4D**). These results are in good agreement with the Northern blot experiments (**Figure 4A** and **Supplementary Figure 3**) and further support that Rho-dependent attenuators sensitive to cold regulate *cspA*, *cspB*, and *cspG*.

The increases of RT-qPCR signals upon cold shock were smaller for *nsrR* and *rnr*, as were the differences between *rho*$^{+}$ and *rho*^{R66S} signals at 37°C (**Figure 4D**). These differences were further reduced but not fully abrogated at 15°C ($p < 10^{-2}$, unpaired, two-tailed Student's t-tests), which is also consistent with Northern blot observations (**Figure 4B**). Thus, Rho-dependent attenuation appears to be less important for the temperature-dependent regulation of the *nsrR* and *rnr* genes than for *cspA*, *cspB*, and *cspG*. Alternatively, a temperature lower than 15°C may be required to fully switch off Rho-dependent attenuation of the *nsrR-rnr-yjfHI* operon. Interestingly, RT-qPCR probing of *lpxP* suggests that this gene is also regulated by Rho in a temperature-dependent manner (**Figure 4D**) even though *in vitro* Rho-dependent termination in *lpxP* is not strongly affected by temperature (**Figure 3E**). *In vivo*, however, the intragenic *lpxP* terminator (**Figures 2B** and **3E**) should be regulated by cold-shock

stimulated *lpxP* translation.[4] Increased translation may also better protect the *lpxP* mRNA from degradation by ribonucleases, thereby further contributing to the higher level of the mRNA at 15°C versus 37°C (**Figure 4D**).

Taken together, our *in vitro* and *in vivo* data reveal a new facet of the intricate regulation of cold-shock genes based on the modulation of Rho-dependent attenuation. Two alternative mechanisms appear to be involved. On one hand, an increase in the efficiency of translation upon cold shock contributes to shield intragenic *Rut* sites from Rho action (e.g. as for *lpxP* and, possibly, *rnr*; **Figure 1**, top left). On the other hand, an increase in the secondary structure of the mRNA at the lower temperature prevents Rho access to a *Rut* site located in the 5'-leader portion of the mRNA (e.g. as for *cspA*, *cspB*, and *cspG*; **Figure 1**, top right).

Mutations that stabilize the cold-shock conformation of the cspA mRNA leader inhibit Rho-dependent attenuation

Paralogs corresponding to six of the nine Csp proteins found in *E. coli* are also present in *Salmonella enterica*. Notably, *Salmonella* CspA shares 100% identity with its *E. coli* counterpart, and the two genes exhibit a 91% identity in their 5'UTRs, which are 164 and 160 nt long, respectively (**Supplementary Figure 4A**). Drawing from the analogy with *E. coli*, where the structure of the 5'UTR of *cspA* was determined by DMS mapping *in vivo*[4], the *Salmonella cspA* sequence is predicted to adopt two alternative conformations: a more 'open' conformation at 37°C and a folded one containing a long hairpin-like structure at lower temperature (**Supplementary Figure 4B**). Conceivably, the latter structure might sequester residues required for Rho binding and thus promote readthrough transcription following the cold shock.

To evaluate the role of Rho in the cold-shock regulation of *cspA* in *Salmonella*, we engineered a strain carrying a second copy of the 5'UTR of *cspA* fused to the coding sequence of the *lacZ* gene (in a *lacY*$^+$ background) at an ectopic location under the control of the TetR-regulated P^{tet} promoter. An isogenic derivative of this strain carrying *rho* allele Y80C, which causes a termination defect at *Rut* sites[43,51], was subsequently constructed through phage P22 transduction. Measurement of β-galactosidase activity 30 minutes (**Figure 5A**) and 180 minutes (**Figure 5B**) after the addition of the P^{tet} inducer, anhydrotetracycline (AHTc), revealed

a significant increase in *lacZ* expression caused by the Rho mutation at 37°C, but not at 15°C (**Figures 5A** and **5B**). This is consistent with the *cspA* leader sequence containing a Rho-dependent terminator active only at 37°C. Notably, the mutant-to-wild-type expression ratio at 37°C exhibited a gradual rise during the 30 to 180-minute interval (from approximately 4-fold to 30-fold), suggesting that termination efficiency is enhanced when the bacteria enter stationary phase. Enhanced termination can explain the early finding that *cspA* mRNA levels undergo an abrupt decline in *E. coli* cells transitioning from mid-to-late exponential growth, as reported in early studies.[13,14]

The P^{tet} promoter fusion utilized in these experiments contains only one of the two operator sequences normally found at the 5' end of the *tetA* gene (see Materials and Methods for details).[52] Consequently, TetR-mediated repression exhibits some degree of "leakiness", resulting in low-level transcription in the absence of the inducer. However, due to termination in the *cspA* leader region, expression of the *cspA-lacZ* fusion at 37°C is insufficient to support bacterial growth on a medium containing lactose as the sole carbon source. As a result, the strain is Lac^-. The introduction of the rho^{Y80C} mutation confers a Lac^+ phenotype, most likely by allowing transcription to read through the *cspA* leader region (**Figure 5C**). This observation suggested that the lactose-based medium could be used to positively select mutants evading Rho-dependent termination in the rho^+ background. Colonies growing on minimal lactose plates (see example in **Figure 5C**, upper left spot) were isolated and characterized. This led to the identification of four mutants carrying single base-pair substitutions in the 5'UTR of *cspA*: C41A, A55G, C73U, and C76U. Remarkably, all four changes allow additional base pairing in the hairpin structure predicted to form at low temperature, thereby stabilizing the structure (**Figure 5D** and **Supplementary Figure 4B**).

Measurements of *lacZ* expression in strains carrying each of the four *cspA* alleles alone or in combination with rho^{Y80C} confirmed the *cspA* changes to be completely epistatic to the Rho mutation, indicating that they act in the same pathway as Rho (**Figures 5E** and **5F**). This supports the conclusion that the changes in the *cspA* leader RNA prevent Rho from terminating transcription at 37°C because they enable the hairpin structure to form at this higher temperature.

We selected two of the mutations, C41A and A55G, for further characterization *in vitro*. We prepared ^{32}P-labeled *Salmonella cpsA* leader transcripts carrying either mutation, no

mutation (WT), or the G54U substitution expected to destabilize rather than stabilize the hairpin structure (**Supplementary Figure 4B**). We probed the transcript conformations by native polyacrylamide gel electrophoresis (PAGE). The C41A and A55G transcripts migrated faster in the PAGE gel than the WT transcript (**Supplementary Figure 5A**), indicating more compact conformations consistent with the stabilization of the hairpin structure by the mutations. By contrast, the G54U mutation markedly reduced the electrophoretic mobility of the transcript, consistent with a more open conformation enacted by hairpin destabilization. Furthermore, we observed different *in vitro* transcription termination profiles with DNA templates encoding the WT *Salmonella cpsA* or mutant sequences. Notably, in defined conditions, the WT and G54U sequences could sustain premature Rho-dependent termination in the 5'UTR whereas the C41A and A55G mutant sequences could not (**Supplementary Figure 5B**), thereby linking termination efficiency to the stability of the leader hairpin structure. Thus, both our *in vitro* and *in vivo* observations support the conclusion that the temperature-dependent folding pathway of the *cspA* mRNA leader not only governs *cspA* translation[4,9] but also finely controls Rho-dependent attenuation of *cspA* expression.

CspA stimulates Rho-dependent termination at csp terminators

Since CspA contributes to regulate cold shock genes (including *cspA* itself) during cold acclimation, we wondered if this could proceed, at least in part, through the modulation of Rho-dependent attenuation. To test this possibility, we performed *in vitro* transcription experiments in the presence of CspA. As noted above, we first tested a concentration (0.5 µM) just below the dissociation constants measured for CspA with model oligonucleotides at 20°C (1-10 µM range).[12,21] At this sub-saturating concentration, CspA had no effect on Rho-dependent transcription termination with the tested DNA templates at both 15°C and 37°C (**Figure 3**). Results were different when we tested CspA at its concentration in cold-shocked cells (~100 µM).[22] At this high (saturating) concentration, CspA was able to both stimulate Rho-dependent termination and activate upstream termination sites (**Figure 6A, B** and **Supplementary Figure 2B-D**).

The upstream shift of the termination window was particularly marked with the *cspA* template for which Rho-dependent termination prevailed in the 5'UTR or farther in the CDS in presence or absence of CspA, respectively (**Figure 6A**). Although these features are

reminiscent of the action of NusG, in particular at suboptimal Rho-dependent terminators[37,41-43], CspA and NusG appear to have additive rather than mutually exclusive effects (**Figure 6A, B** and **Supplementary Figure 2B-D**). More importantly, CspA was able to activate Rho-dependent termination at 15°C with the *csp* templates and at the upstream *nsrR* terminator, this activation being particularly efficient when NusG is also present (**Figure 6A, B** and **Supplementary Figure 2B, D**). CspA had a more modest effect at the *rnr*, *lpxP*, and control λtR1 terminators and did not shift or enlarge the termination window in these cases (**Figure 6C** and **Supplementary Figure 2A, C**). Thus, CspA (and possibly other Csp) can stimulate Rho-dependent termination *in vitro*, presumably by disrupting RNA structures that block Rho access to *Rut* sites (**Figure 1**). This effect seems particularly relevant for cold shock genes as it could contribute to the dynamic regulation of their expression during cold acclimation.

To test this hypothesis in bacterial cells, we performed Northern blots and RT-qPCR analyses of the *cspA* mRNA levels in the *rho*$^{+}$ and *rho*^{R66S} strains at different times during the cold acclimation phase. Both analyses confirmed that Rho-dependent attenuation of *cspA* is switched off shortly after cold shock, resulting in similarly high mRNA levels in both *rho*$^{+}$ and *rho*^{R66S} strains (**Figure 6D**, compare 0 h and 0.5 h time points). After 1 h at 15°C, however, *cspA* mRNA became less abundant in the *rho*$^{+}$ strain than in the *rho*^{R66S} mutant and this difference remained significant after 2 h of incubation at 15°C despite the decrease in *cspA* mRNA levels in both strains (**Figure 6D**). After 5 h of incubation at 15°C, *cspA* mRNA levels were even lower and the difference between *rho*$^{+}$ and *rho*^{R66S} strains was no longer statistically significant. These data are consistent with Rho-dependent attenuation of *cspA* being reactivated during the cold acclimation phase, a process that is correlated to the sharp increase of the concentrations of Csp proteins during this phase[3,4,22] and that is congruent with our *in vitro* observations (**Figure 6A**). Thus, the sequential but antagonistic effects of cold temperature and Csp action on the Rho-dependent attenuator of *cspA* trigger a burst of *cspA* expression upon cold shock (~70-fold burst for *rho*$^{+}$ cells; **Figure 6D**).[47] By contrast, *cspA* expression decreases if the exponentially growing cells remain at 37°C (**Supplementary Figure 6**)[13,14], an effect that we ascribe to increased termination by Rho (see discussion of **Figure 5A, B** above), further accentuating the difference between the low and high temperature situations (compare WT levels in **Figures 5A** and **5B** or in **Figures 4A, D** and **6D**).

CONCLUSIONS

Growing evidence marks Rho-dependent termination of transcription as a pivotal mechanism in the bacterial response to environmental changes and stresses. Relevant examples involve Rho in the response to genotoxic and oxidative stresses[53,54], exposure to toxic substances such as copper[55] or antibiotics[56], nutriment fluctuations[37,43] or variations in the levels of key metabolites[36,45,57-61], and even in the synthesis of the general stress sigma factor RpoS.[62] Rho involvement often hinges on a Rho-dependent terminator whose efficiency is tuned by a specific cytoplasmic signal affecting the structure or translatability of the mRNA (**Figure 1**). Notably, Rho-dependent regulatory mechanisms have been linked to the dynamic remodeling of mRNA leader regions upon binding of small molecule ligands[36,63], regulatory small RNAs[43,62], and proteins.[37] Here, we provide evidence that a physical signal – temperature – can also remodel Rho access to mRNAs and regulate transcription termination.

Our data unveil the existence of thermosensing Rho-dependent terminators in the 5'UTRs of transcripts encoding key CSR proteins, namely CspA, CspB, CspG, and Rnase R. The transcription terminators are functional at 37°C and contribute to repress the synthesis of the CSR proteins alongside the known posttranscriptional mechanisms (**Figure 7**, left). Upon a temperature downshift, extensive restructuring of the 5'-leader of the mRNA, which is well documented for *cspA* and *cspB*[4,9], hinders Rho action and allows transcription to proceed into the structural genes (**Figure 7**, right). Once the Csp proteins have reached a sufficiently high concentration, binding of these proteins to the mRNA brings the 5'-leader back to a silencing-prone conformation. This negative feedback mechanism down-regulates *csp* expression at both transcriptional and posttranscriptional levels during the acclimation phase (**Figure 7**).

Previous work supports the implication of transcriptional regulation in the CSR. Early studies suggested that *cspA* transcription is regulated by sequences present in the leader portion of the gene and by the interaction of the 5'-leader RNA with Csp proteins[17,18,23,24,47], although the exact mechanism remained unidentified. More recently, genome-wide studies unveiled Rho-dependent signals in the 5'UTRs and CDSs of genes/operons involved in the CSR, including *CspA* (**Figure 2A**).[26,27,38] Besides the representative cases studied here, genome-wide studies suggest that several other CSR genes could be regulated in a Rho-dependent manner (**Table S4**). This regulation may be based on RNA thermosensors located in 5'-leaders, as it is the case for *cspA/B/G* genes (**Figure 7**) or on intragenic *Rut* sites whose accessibility is

modulated by the efficiency of translation, as for *lpxP* (see above). The presence of *Rut* peaks upstream from the promoters of some CSR genes (**Table S4**) suggests an additional, yet untested scenario whereby regulation would stem from read-through of terminators that normally insulate upstream transcription units (i.e. thermosensing terminators located in mRNA 3'UTRs).

The regulation of *rpoS* by the cold-induced sRNA DsrA[64] provides another compelling example of a Rho-dependent switch operating during cold acclimation. Indeed, DsrA binding to the 5'-leader of *rpoS* enhances the translatability of the mRNA at low temperature[65] but also inhibits Rho-dependent attenuation of *rpoS*.[62] The latter is likely to contribute to the increased expression of *rpoS* at low temperatures.[66] Conversely, one might envision that activation of Rho-dependent termination participates in the repression of non-CSR proteins upon cold shock. Translational repression associated to the increased structuring of bulk mRNA[4] is thought to trigger widespread decoupling of translation from transcription.[32,33] Whether this favors Rho-dependent termination (contributing to gene silencing) or is compensated by increased structural shielding of intragenic *Rut* sites (**Figure 1**) awaits experimental testing. Regardless, the work described here defines Rho-dependent transcription termination as an important component of the bacterial response to cold stress and sets a new paradigm for how RNA remodeling by antagonistic factors, here temperature and Csp chaperones, can modulate transcription termination.

MATERIALS AND METHODS

Materials

Unless specified otherwise, chemicals and enzymes were from Merck and New England Biolabs, respectively. Radionucleotides were obtained from PerkinElmer and synthetic oligonucleotides (**Table S1**) from Eurogentec or Merck.

DNA templates for *in vitro* transcription were prepared by standard PCR amplification of genomic DNA[67] with the forward (fwd) and reverse (rev) primer pairs listed in **Table S1**. In a second round of PCR, the forward primer was replaced by primer T7A1_univ or pT7-univ_A to introduce the full sequence of the T7 φ6.5 (for T7 transcription) or T7A1 promoter (for transcription with *E. coli* RNAP), respectively. Sequences of the DNA templates are provided in **Table S3**.

Plasmid pET28b-CspA was obtained by subcloning the *E. coli cspA* CDS between the NcoI and XhoI sites of plasmid pET28b(+) (Novagen). The CspA protein was overexpressed in BL21(DE3) cells harboring the pET28b-CspA plasmid and purified as described previously.[68] The Rho and NusG proteins were prepared as described previously. [67] Rho concentrations are expressed in hexamers throughout.

Bacterial strains and growth conditions

Bacterial strains are listed in **Table S2**. *E. coli* MG1655 *rho*$^{+}$ and *rho*^{R66S} strains were kindly provided by Pr. Joseph T. Wade (New York state University at Albany). *Salmonella* strains are described in the next sections. For cold shock experiments, bacteria were cultured in LB broth at 37°C until absorbance at 600 nm (A_{600}) reached 0.5. Culture aliquots (50 mL) were then withdrawn and either kept at 37°C or transferred to a 15°C water bath. Cultures were further incubated at 37°C or 15°C for the indicated times.

Construction of an ectopic *cspA-lacZY* fusion in *Salmonella*

Salmonella strain MA14009 harbors a tripartite *tetR*-P^{tet}-*ccdB-cat* cassette[69] inserted in the region upstream of the *chiPQ* promoter in the background of *chiP-lacZY* translational fusion.[43] This strain was made recombineering-proficient by introduction of lambda *Red* plasmid pKD46.[70] The resulting strain was transformed with a DNA fragment spanning the *cspA* leader region amplified from wild-type *Salmonella* with primers AN13 and AN16 (**Table S1**). These primers carry 5' extensions designed to recombine within the P^{tet} promoter region on one end (AN13), and with the sequence immediately downstream from the initiation codon of *lacZ* on the opposite end (AN16), so as to replace the entire segment between P^{tet} and the beginning of *lacZ* open reading frame, with the *cspA* sequence. Recombinants were obtained selecting for AHTc-resistance as described.[69] One of these recombinants, strain MA14627, which thus carries the 5'UTR of *cspA* directly fused to the *lacZY* operon under the control of the *tetR*-P^{tet} module was used for the experiments described here.

Isolation of *Salmonella cspA* leader mutants

Two cultures of strain MA14627 inoculated from separate single colonies were grown overnight at 37°C. 0.1 ml aliquots were spread on the surface of two minimal (NCE) lactose plates[43], and incubated at 37°C. Lac^{+} colonies typically developed during a 36-to-48-hour

incubation. A number of colonies were picked, purified by streaking, and subjected to colony PCR (primers ppZ18 – AB24). The amplified fragments were subjected to Sanger sequencing. Out of 14 clones analyzed, 7 carried changes in the *cspA* leader sequence: the four point-mutants characterized in this study, C41A, A55G, C73U (three occurrences), C76U and one carrying the deletion of the first 80 bp of the 5'UTR. The latter was not analyzed any further.

RNA extraction and Northern blot analyses

Total RNA was extracted from *E. coli* cell cultures by the acid hot phenol procedure as described previously[71], with minor modifications. Briefly, bacterial cultures were mixed with one tenth of volume of ice cold Ethanol:Phenol [95:5] solution to quench RNA degradation. Bacteria were pelleted, suspended in RNA extraction buffer (20 mM sodium acetate pH 5.2, 2% SDS, and 0.3 M sucrose), and boiled for 2 min. The mixtures were mixed with one volume of acidic phenol, left at room temperature for 30 sec, and incubated on ice for 2 min. Mixtures were then centrifuged at 12,000 g for 5 min. The aqueous phases were collected and extracted thrice with a solution of Phenol:Chloroform:Isoamyl Alcohol [25:24:1] and twice with chloroform. RNA preparations were purified on RNA Clean & Concentrator-25 columns following manufacturer (Zymo Research) instructions and stored at -20°C in ME buffer (10 mM MOPS, PH 6.5, 1 mM EDTA) before use. For Northern blotting, total RNA was fractionated on a denaturing 8 % polyacrylamide/urea gel or a 1.5 % agarose MOPS/formaldehyde gel and electro-transferred to a Hybond-N^+ membrane (Cytiva). Blots were hybridized to ^{32}P-end labeled DNA oligonucleotide probes complementary to the mRNA region of interest and to 5S ribosomal RNA (**Table S1**). Hybridization signals were detected by phosphorimaging with a Typhoon FLA-9500 instrument equipped with ImaqeQuant TL v8.1 software (Cytiva). Signals for the 5S rRNA were used for normalization of the mRNA signals.[37]

Reverse transcription-quantitative PCR (RT-qPCR) analyses

Residual DNA was removed from RNA samples by treatment with Turbo DNase I (Thermo Fisher Scientific), following manufacturer's instructions. Then, 0.5 µg of total RNA was used for cDNA synthesis with 2.5 µM random hexamer primer, 0.5 mM of each dNTP, and 200 U of Maxima H-minus reverse transcriptase (Thermo Fisher Scientific) upon incubation for 5 min at 25°C and 1 h at 50°C. For quantitative PCR, each cDNA was mixed with the Power SYBR® Green PCR Master Mix (Applied Biosystems™) and forward and reverse primers (0.2 µM each; **Table**

S1). Mixtures were placed in a LightCycler®480 qPCR instrument (Roche) and amplified with the following conditions: initial denaturation at 95°C for 10 min followed by 40 cycles of 15 s of denaturation at 95°C, and 1 min of hybridization/elongation at 60°C. Sample melting curves were used to monitor the specificity of cDNA amplification at each cycle. The threshold cycle 'Ct' was calculated with the instrument software (LightCycler®480 v1.5.0) using the second derivative maximum method. Data analysis was performed by the relative standard curve method, as recommended in Applied Biosystems User Bulletin #2. Sample signals were then normalized using *rrsB* (which encodes 16S rRNA).[61] Statistical analyses were performed with Kaleidagraph 4.1 (Synergy software) using the unequal variance option of the unpaired two-tailed Student's t-test.

Measurement of β-galactosidase activity

β-galactosidase activity was assayed in toluene-permeabilized *Salmonella* cells as described by Miller[72] and is expressed in Miller units. All measurements were performed three times, each time on duplicate cultures, as specified in the legend to Figure 5. Statistical significance was determined as specified in the legend to Figure 5 using GraphPad Prism 9 software.

Transcription termination experiments

Standard transcription termination experiments were performed as described[40], with minor modifications. Briefly, DNA template (0.1 pmol), *E. coli* RNAP (0.3 pmol), Rho (1.4 pmol), NusG (0 or 2.8 pmol), Superase-In (0.5U/µL), and CspA (0, 10, or 2000 pmol) were mixed in 18 µL of transcription buffer (20 mM HEPES, pH 7.5, 150 mM potassium acetate, 10 mM NaCl, 100 nM $CaCl_2$, 5 mM $MgCl_2$, 1,5 mM DTT) and incubated for 10 min at 37°C. Then, 2 µL of initiation mix (2 mM ATP, GTP, and CTP, 0.2 mM UTP, 2.5 µCi/µL of ^{32}P-αUTP, and 250 µg/mL rifampicin in transcription buffer) were added to reaction mixtures before incubation for 20 min at 37°C. Transcription reactions were stopped with 4 µL of EDTA (0.5 M), 6 µL of tRNA (0.25mg/mL), and 80 µL of sodium acetate (0.42 M) before extraction with a phenol:chloroform:isoamyl alcohol [25:24:1] mixture and precipitation at -20°C with 330 µL of ethanol. Reaction pellets were dissolved in denaturing loading buffer (95% formamide, 5 mM EDTA), and analyzed by denaturing 8% PAGE and Typhoon FLA-9500 phosphorimaging.

Electrophoretic mobility shift assay (EMSA)

DNA templates encoding the wild-type mRNA leader of *Salmonella cspA* (nt 1-164) and single-point mutants C41A, A55G, and G54U were transcribed with T7 RNA polymerase as described previously[73], in the presence of ^{32}P-αUTP. The ^{32}P-labeled transcripts were purified by denaturing 8% PAGE and stored at -20°C in ME buffer. Trace amounts (~400 β-ray counts per minute) of each transcript were dissolved in EMSA buffer (10 mM MOPS, pH 6.5, 1 mM EDTA, and either 50 mM KCl or 150 mM potassium acetate) and incubated for 3 min at 95°C and then for 15 min at 37°C. Samples were mixed with Ficoll-400 (8% v/v final) and analyzed by native 6% PAGE (4 h migration at 20°C and 10 V/cm) and Typhoon FLA-9500 phosphorimaging.

Bioinformatics analyses

Percentages of C and G residues along the *E. coli* MG1655 genome were computed with EMBOSS freak 5.0.0 (step: 1; averaging window: 78) and visualized with Kaleidagraph 4.1. Log_{10} fold enrichment (FE) profiles were determined from Helicase-SELEX data[38] deposited in the European Nucleotide Archive under accession #PRJEB50170. Curated reads were mapped on the MG1655 genome (NC_000913.3) with Bowtie2 (v2.4.2, default options). Coverage and RPM normalization were performed with Bedtools v2.29.2. The Log_{10}FE profiles were obtained with MACS2 bdgcmp v2.1.1 using the deposited R10+ (+NusG) or R10- (-NusG) sample as input and R0 sample as control. Peak calling was performed with MACS2 bdgpeakcall v2.1.1 (cutoff: 0; Min peak length: 30; Max gap: 30). Log_{10}FE profiles were visualized with the JBrowse genome browser (jbrowse.org).[74]

AUTHOR CONTRIBUTIONS

MD performed Northern blot, RT-qPCR, and *in vitro* transcription experiments; NF-B constructed the *Salmonella* strains used in this study; TDD prepared DNA templates and performed Northern blot and EMSA experiments; PK and LB performed β-galactosidase assays; EE and MB performed computational mining of published Helicase-SELEX and genomic data; LB isolated *Salmonella cspA* leader mutants; MB prepared proteins and wrote the paper with help from MD, NF-B, and LB; MD, NF-B, LB, and MB conceived the study. All authors participated in data analysis.

AKNOWLEDGMENTS

N.F-B, LB, and MB acknowledge support from the French Centre National de la Recherche Scientifique (CNRS). This work was also supported by grants from Agence Nationale de la Recherche (ANR) to M.B. (ANR-15-CE11-0024-2 and ANR-19-CE44-0009-01).

COMPETING INTERESTS

The authors declare no competing interests

FIGURE LEGENDS

Figure 1: Rho-dependent termination. Rho binds to free *Rut* sites within nascent transcripts and then uses its ATP-dependent motor activity to catch up with RNA polymerase (RNAP) along the RNA chain and to trigger the dissociation of the transcription elongation complex (bottom).[75] Rho action is prevented by the presence of translating ribosomes or by secondary structures in the nascent transcript that block *Rut* sites (top). In an alternative termination pathway, Rho binds RNAP early on during transcription and detects accessible *Rut* sites in the nascent transcript from this RNAP-bound position[76], which is not represented here for simplicity.

Figure 2: Putative *Rut* sites in the 5'-UTRs of *E. coli* genes involved in the CSR. **(A)** Fold enrichment (FE; $\log_{10}$ scale) profiles for Helicase-SELEX experiments performed with Rho in presence or absence of NusG were determined from published data.[38] Cyan bars highlight the positions of the enrichment peaks (median $\log_{10}$FE ≥ 0.3) suggestive of *Rut* sites in the 5'UTRs. Regions where transcription is upregulated *in vivo* in presence of the Rho inhibitor Bicyclomycin, as determined by ChIP-chip (orange arrows)[27] or microarrays and RNAseq (purple bars)[26] are also shown. Note that different scales along the genome coordinates (x-axis) are used for the various panels. **(B)** C>G bubbles (black arrows) overlap with the *Rut* peaks detected by Helicase-SELEX (cyan lines) and are present upstream from the *in vitro* transcription termination regions (brown lines), a feature characteristic of Rho-dependent terminators. Percentages of C and G residues were calculated using a sliding window of 78 nt. Termination boundaries were estimated with the molecular size calibration/calculation function of ImageQuant software using all *in vitro* transcription gel lanes.

Figure 3: Cold shock genes contain Rho-dependent terminators in their 5'UTRs. Representative gel images show the *in vitro* transcription profiles obtained with DNA templates encoding the upstream sections of the *E. coli cspA*, *cspB*, *cspG*, *lpxP* and *nsrR* transcription units (**A-E**) or the λtR1 terminator (**F**). Transcription reactions were performed at 15 or 37°C with or without Rho (20 nM), NusG (70 nM), or CspA (0.5 µM), as indicated. Bands corresponding to runoff (RO) and termination (Term) transcripts are indicated. Since transcripts are labeled by incorporation of α^{32}P-UTP during transcription, band intensities

reflect both the amounts and sizes of the transcripts. A downstream *nsrR* termination site (*) is detected at 15°C (panel D).

Figure 4: Transcription of cold shock genes is regulated by Rho *in vivo*. *E. coli* log phase cultures (A_{600} = 0.5) were incubated for 30 min at 15°C or 37°C before RNA extraction. (**A, B**) Northern blot analysis of the expression of *cspA* and *nsrR* in WT (*rho*$^{+}$) and *rho*^{R66S} (R66S) strains. Phosphorimager *cspA* counts were normalized to 5S RNA and the resulting values were divided by that obtained for WT at 37°C. The [*cspA*] values are (mean ± SD) values from three independent biological replicates. Pairwise comparisons of the normalized WT and R66S signals along gel lanes are provided on the right of the *cspA* membrane images (FL: full-length transcripts). Polycistronic *nsrR-rnr-yjfHI* transcripts are subjected to complex posttranscriptional processing[5,6] and were not quantified. (**C, D**) RT-qPCR confirms Rho-dependent regulation of cold shock genes. For each gene, signals are normalized to the condition *rho*$^{+}$, 37°C. Four biological replicates were analyzed by RT-qPCR, each time in triplicate (open circles represent the triplicate means). Statistical significance was determined by unpaired two-tailed Student's t-tests (ns, $p > 0.05$; *, $p < 0.05$; **, $p < 10^{-2}$; ***, $p < 10^{-3}$; ****, $p < 10^{-4}$).

Figure 5. Mutations in the *cspA* leader RNA prevent Rho-dependent transcription termination in *Salmonella*. (**A, B**) Impact of Rho mutation Y80C on *cspA-lacZY* expression. Isogenic strains carrying the *cspA-lacZY* fusion under control of the P^{tet} promoter and either *rho*$^{+}$ or *rho*^{Y80C} were cultured in LB at 37°C until reaching mid-exponential phase (DO_{600} ≈ 0.4 - 0.5). At this point, expression of the *cspA-lacZY* fusion was induced by adding the P^{tet} inducer AHTc. The cultures were then divided, with one half transferred to 15°C and the other maintained at 37°C, and both were further incubated for (**A**) 30 and (**B**) 180 min. Cells were then processed for the determination of β-galactosidase activity. (**C**) Lac phenotype of strains carrying the P^{tet}-*cspA-lacZY* fusion in combination with either *rho*$^{+}$ (strain MA14635) or *rho*^{Y80C} (strain MA14636). Bacteria were cultured to stationary phase and 10 µl were spotted on minimal-lactose plates ±AHTc (37°C). The strain carrying *rho*^{Y80C} is Lac^{+} under non-inducing conditions (-AHTc) whereas the *rho*$^{+}$ strain is Lac^{-}. The yellow arrow highlights a Lac^{+} colony forming of the lawn of *rho*$^{+}$ cells. (**D**) Position of mutations suppressing the inhibitory effect of Rho on

640 *cspA-lacZ* expression at 37°C . (**E, F**) Effect of the mutations in **D** on the expression of the *cspA-*
641 *lacZ* fusion in the presence or absence of Rho Y80C at 37°C (**E**) and at 15°(**F**). Cells were
642 cultured and treated as described in (**A, B**) with a time of incubation of 30 min after AHTc
643 induction. Throughout this experiment, β-galactosidase activity was assayed with the method
644 of Miller[72] on three independent replicates of the bacterial cultures, with each assay carried
645 out in duplicate. Statistical significance was determined by one-way ANOVA with Šidák's
646 multiple comparisons test (ns, $p > 0.05$; ***, $p \leq 10^{-3}$; ****, $p \leq 10^{-4}$).
647
648 **Figure 6:** A high concentration of CspA stimulates Rho-dependent termination at *E. coli csp*
649 terminators. Transcription experiments were performed with the *cspA* (**A**), *cspB* (**B**) and
650 control λ*tR1* (**C**) DNA templates as described in the legend to Figure 3, except that a 200-fold
651 higher concentration of CspA was used (100 vs 0.5 µM). (**D**) Northern blot and RT-qPCR
652 analyses of Rho-dependent attenuation of *cspA* as a function of the duration of the incubation
653 at 15°C following cold shock. Four biological replicates were analyzed by RT-qPCR, each time
654 in triplicate (open circles represent the triplicate means). Statistical significance was
655 determined by unpaired two-tailed Student's t-tests (ns, $p > 0.05$; *, $p < 0.05$; **, $p < 10^{-2}$; ***,
656 $p < 10^{-3}$).
657
658 **Figure 7:** Model for regulation of *csp* genes. (**Left**) Rho-dependent attenuation of transcription
659 in the 5'UTR inhibits *csp* expression at 37°C. Poor translatability of the transcripts that escape
660 termination further contributes to *csp* down-regulation directly[4,9,10] and, possibly indirectly,
661 by facilitating intragenic transcription termination or RNA degradation or both.[7] (**Right**)
662 Restructuring of the 5'-leader upon the cold shock hides the *Rut* site and prevents premature
663 transcription termination, at the same time enhancing the accessibility of the ribosome
664 binding site. Protection of the CDS by translating ribosomes may contribute to stabilize the
665 mRNA. During cold acclimation, the concentration of Csp proteins increases until it becomes
666 sufficient to promote Csp binding to the mRNA. Csp binding drives the mRNA into a
667 conformation that resembles the "37°C-conformation"[4] and thereby restores attenuation.

REFERENCES

1. Barria, C., Malecki, M., and Arraiano, C.M. (2013). Bacterial adaptation to cold. Microbiology (Reading) *159*, 2437-2443. 10.1099/mic.0.052209-0.
2. Zhang, Y., and Gross, C.A. (2021). Cold Shock Response in Bacteria. Annual review of genetics *55*, 377-400. 10.1146/annurev-genet-071819-031654.
3. Gualerzi, C.O., Giuliodori, A.M., and Pon, C.L. (2003). Transcriptional and post-transcriptional control of cold-shock genes. J Mol Biol *331*, 527-539. 10.1016/s0022-2836(03)00732-0.
4. Zhang, Y., Burkhardt, D.H., Rouskin, S., Li, G.W., Weissman, J.S., and Gross, C.A. (2018). A Stress Response that Monitors and Regulates mRNA Structure Is Central to Cold Shock Adaptation. Mol Cell *70*, 274-286 e277. 10.1016/j.molcel.2018.02.035.
5. Cairrao, F., Cruz, A., Mori, H., and Arraiano, C.M. (2003). Cold shock induction of RNase R and its role in the maturation of the quality control mediator SsrA/tmRNA. Mol Microbiol *50*, 1349-1360. 10.1046/j.1365-2958.2003.03766.x.
6. Cairrao, F., and Arraiano, C.M. (2006). The role of endoribonucleases in the regulation of RNase R. Biochem Biophys Res Commun *343*, 731-737. 10.1016/j.bbrc.2006.03.040.
7. Fang, L., Jiang, W., Bae, W., and Inouye, M. (1997). Promoter-independent cold-shock induction of cspA and its derepression at 37 degrees C by mRNA stabilization. Mol Microbiol *23*, 355-364. 10.1046/j.1365-2958.1997.2351592.x.
8. Goldenberg, D., Azar, I., and Oppenheim, A.B. (1996). Differential mRNA stability of the cspA gene in the cold-shock response of Escherichia coli. Mol Microbiol *19*, 241-248. 10.1046/j.1365-2958.1996.363898.x.
9. Giuliodori, A.M., Di Pietro, F., Marzi, S., Masquida, B., Wagner, R., Romby, P., Gualerzi, C.O., and Pon, C.L. (2010). The cspA mRNA is a thermosensor that modulates translation of the cold-shock protein CspA. Mol Cell *37*, 21-33. 10.1016/j.molcel.2009.11.033.
10. Yamanaka, K., Mitta, M., and Inouye, M. (1999). Mutation analysis of the 5' untranslated region of the cold shock cspA mRNA of Escherichia coli. J Bacteriol *181*, 6284-6291. 10.1128/JB.181.20.6284-6291.1999.
11. Goldstein, J., Pollitt, N.S., and Inouye, M. (1990). Major cold shock protein of Escherichia coli. Proc Natl Acad Sci U S A *87*, 283-287. 10.1073/pnas.87.1.283.
12. Giuliodori, A.M., Belardinelli, R., Duval, M., Garofalo, R., Schenckbecher, E., Hauryliuk, V., Ennifar, E., and Marzi, S. (2023). Escherichia coli CspA stimulates translation in the cold of its own mRNA by promoting ribosome progression. Front Microbiol *14*, 1118329. 10.3389/fmicb.2023.1118329.
13. Brandi, A., Spurio, R., Gualerzi, C.O., and Pon, C.L. (1999). Massive presence of the Escherichia coli 'major cold-shock protein' CspA under non-stress conditions. EMBO J *18*, 1653-1659. 10.1093/emboj/18.6.1653.
14. Brandi, A., and Pon, C.L. (2012). Expression of Escherichia coli cspA during early exponential growth at 37 degrees C. Gene *492*, 382-388. 10.1016/j.gene.2011.10.047.
15. Xia, B., Ke, H., Jiang, W., and Inouye, M. (2002). The Cold Box stem-loop proximal to the 5'-end of the Escherichia coli cspA gene stabilizes its mRNA at low temperature. J Biol Chem *277*, 6005-6011. 10.1074/jbc.M109700200.
16. Etchegaray, J.P., and Inouye, M. (1999). Translational enhancement by an element downstream of the initiation codon in Escherichia coli. J Biol Chem *274*, 10079-10085. 10.1074/jbc.274.15.10079.
17. Fang, L., Hou, Y., and Inouye, M. (1998). Role of the cold-box region in the 5' untranslated region of the cspA mRNA in its transient expression at low temperature in Escherichia coli. J Bacteriol *180*, 90-95. 10.1128/JB.180.1.90-95.1998.
18. Bae, W., Jones, P.G., and Inouye, M. (1997). CspA, the major cold shock protein of Escherichia coli, negatively regulates its own gene expression. J Bacteriol *179*, 7081-7088. 10.1128/jb.179.22.7081-7088.1997.

19. Wang, N., Yamanaka, K., and Inouye, M. (1999). CspI, the ninth member of the CspA family of Escherichia coli, is induced upon cold shock. J Bacteriol *181*, 1603-1609. 10.1128/JB.181.5.1603-1609.1999.
20. Jones, P.G., VanBogelen, R.A., and Neidhardt, F.C. (1987). Induction of proteins in response to low temperature in Escherichia coli. J Bacteriol *169*, 2092-2095. 10.1128/jb.169.5.2092-2095.1987.
21. Rennella, E., Sara, T., Juen, M., Wunderlich, C., Imbert, L., Solyom, Z., Favier, A., Ayala, I., Weinhaupl, K., Schanda, P., et al. (2017). RNA binding and chaperone activity of the E. coli cold-shock protein CspA. Nucleic Acids Res *45*, 4255-4268. 10.1093/nar/gkx044.
22. Jiang, W., Hou, Y., and Inouye, M. (1997). CspA, the major cold-shock protein of Escherichia coli, is an RNA chaperone. J Biol Chem *272*, 196-202. 10.1074/jbc.272.1.196.
23. Fang, L., Xia, B., and Inouye, M. (1999). Transcription of cspA, the gene for the major cold-shock protein of Escherichia coli, is negatively regulated at 37 degrees C by the 5'-untranslated region of its mRNA. FEMS Microbiol Lett *176*, 39-43. 10.1111/j.1574-6968.1999.tb13639.x.
24. Bae, W., Phadtare, S., Severinov, K., and Inouye, M. (1999). Characterization of Escherichia coli cspE, whose product negatively regulates transcription of cspA, the gene for the major cold shock protein. Mol Microbiol *31*, 1429-1441. 10.1046/j.1365-2958.1999.01284.x.
25. Bae, W., Xia, B., Inouye, M., and Severinov, K. (2000). Escherichia coli CspA-family RNA chaperones are transcription antiterminators. Proc Natl Acad Sci U S A *97*, 7784-7789. 10.1073/pnas.97.14.7784.
26. Peters, J.M., Mooney, R.A., Grass, J.A., Jessen, E.D., Tran, F., and Landick, R. (2012). Rho and NusG suppress pervasive antisense transcription in Escherichia coli. Genes Dev *26*, 2621-2633. 10.1101/gad.196741.112.
27. Peters, J.M., Mooney, R.A., Kuan, P.F., Rowland, J.L., Keles, S., and Landick, R. (2009). Rho directs widespread termination of intragenic and stable RNA transcription. Proc Natl Acad Sci U S A *106*, 15406-15411. 10.1073/pnas.0903846106.
28. Cardinale, C.J., Washburn, R.S., Tadigotla, V.R., Brown, L.M., Gottesman, M.E., and Nudler, E. (2008). Termination factor Rho and its cofactors NusA and NusG silence foreign DNA in E. coli. Science *320*, 935-938. 10.1126/science.1152763.
29. Kriner, M.A., Sevostyanova, A., and Groisman, E.A. (2016). Learning from the Leaders: Gene Regulation by the Transcription Termination Factor Rho. Trends Biochem Sci *41*, 690-699. 10.1016/j.tibs.2016.05.012.
30. Bossi, L., Figueroa-Bossi, N., Bouloc, P., and Boudvillain, M. (2020). Regulatory interplay between small RNAs and transcription termination factor Rho. Biochim Biophys Acta Gene Regul Mech *1863*, 194546. 10.1016/j.bbagrm.2020.194546.
31. Bastet, L., Turcotte, P., Wade, J.T., and Lafontaine, D.A. (2018). Maestro of regulation: Riboswitches orchestrate gene expression at the levels of translation, transcription and mRNA decay. RNA biology *15*, 679-682. 10.1080/15476286.2018.1451721.
32. Weber, M.H., and Marahiel, M.A. (2003). Bacterial cold shock responses. Sci Prog *86*, 9-75. 10.3184/003685003783238707.
33. Gowrishankar, J., and Harinarayanan, R. (2004). Why is transcription coupled to translation in bacteria? Mol Microbiol *54*, 598-603.
34. Roberts, J.W. (2019). Mechanisms of Bacterial Transcription Termination. J Mol Biol *431*, 4030-4039. 10.1016/j.jmb.2019.04.003.
35. Boudvillain, M., Figueroa-Bossi, N., and Bossi, L. (2013). Terminator still moving forward: expanding roles for Rho factor. Curr Opin Microbiol *16*, 118-124.
36. Hollands, K., Proshkin, S., Sklyarova, S., Epshtein, V., Mironov, A., Nudler, E., and Groisman, E.A. (2012). Riboswitch control of Rho-dependent transcription termination. Proc Natl Acad Sci U S A *109*, 5376-5381.
37. Figueroa-Bossi, N., Schwartz, A., Guillemardet, B., D'Heygere, F., Bossi, L., and Boudvillain, M. (2014). RNA remodeling by bacterial global regulator CsrA promotes Rho-dependent transcription termination. Genes Dev *28*, 1239-1251. 10.1101/gad.240192.114.

38. Delaleau, M., Eveno, E., Simon, I., Schwartz, A., and Boudvillain, M. (2022). A scalable framework for the discovery of functional helicase substrates and helicase-driven regulatory switches. Proc Natl Acad Sci U S A *119*, e2209608119. 10.1073/pnas.2209608119.
39. Alifano, P., Rivellini, F., Limauro, D., Bruni, C.B., and Carlomagno, M.S. (1991). A consensus motif common to all Rho-dependent prokaryotic transcription terminators. Cell *64*, 553-563. 10.1016/0092-8674(91)90239-u.
40. Nadiras, C., Eveno, E., Schwartz, A., Figueroa-Bossi, N., and Boudvillain, M. (2018). A multivariate prediction model for Rho-dependent termination of transcription. Nucleic Acids Res *46*, 8245-8260. 10.1093/nar/gky563.
41. Burns, C.M., Nowatzke, W.L., and Richardson, J.P. (1999). Activation of Rho-dependent transcription termination by NusG. Dependence on terminator location and acceleration of RNA release. J Biol Chem *274*, 5245-5251.
42. Shashni, R., Qayyum, M.Z., Vishalini, V., Dey, D., and Sen, R. (2014). Redundancy of primary RNA-binding functions of the bacterial transcription terminator Rho. Nucleic Acids Res *42*, 9677-9690. 10.1093/nar/gku690.
43. Bossi, L., Schwartz, A., Guillemardet, B., Boudvillain, M., and Figueroa-Bossi, N. (2012). A role for Rho-dependent polarity in gene regulation by a noncoding small RNA. Genes Dev *26*, 1864-1873. 10.1101/gad.195412.112.
44. Adams, P.P., Baniulyte, G., Esnault, C., Chegireddy, K., Singh, N., Monge, M., Dale, R.K., Storz, G., and Wade, J.T. (2021). Regulatory roles of Escherichia coli 5' UTR and ORF-internal RNAs detected by 3' end mapping. eLife *10*. 10.7554/eLife.62438.
45. Bastet, L., Chauvier, A., Singh, N., Lussier, A., Lamontagne, A.M., Prevost, K., Masse, E., Wade, J.T., and Lafontaine, D.A. (2017). Translational control and Rho-dependent transcription termination are intimately linked in riboswitch regulation. Nucleic Acids Res *45*, 7474-7486. 10.1093/nar/gkx434.
46. Martinez, A., Opperman, T., and Richardson, J.P. (1996). Mutational analysis and secondary structure model of the RNP1-like sequence motif of transcription termination factor Rho. J Mol Biol *257*, 895-908. 10.1006/jmbi.1996.0210.
47. Etchegaray, J.P., Jones, P.G., and Inouye, M. (1996). Differential thermoregulation of two highly homologous cold-shock genes, cspA and cspB, of Escherichia coli. Genes to cells : devoted to molecular & cellular mechanisms *1*, 171-178. 10.1046/j.1365-2443.1996.d01-231.x.
48. Chhabra, S., and Spiro, S. (2015). Inefficient translation of nsrR constrains behaviour of the NsrR regulon in Escherichia coli. Microbiology (Reading) *161*, 2029-2038. 10.1099/mic.0.000151.
49. Chen, C., and Deutscher, M.P. (2010). RNase R is a highly unstable protein regulated by growth phase and stress. RNA *16*, 667-672. 10.1261/rna.1981010.
50. Matsumoto, Y., Shigesada, K., Hirano, M., and Imai, M. (1986). Autogenous regulation of the gene for transcription termination factor rho in Escherichia coli: localization and function of its attenuators. J Bacteriol *166*, 945-958.
51. Bossi, L., Ratel, M., Laurent, C., Kerboriou, P., Camilli, A., Eveno, E., Boudvillain, M., and Figueroa-Bossi, N. (2019). NusG prevents transcriptional invasion of H-NS-silenced genes. PLoS Genet *15*, e1008425. 10.1371/journal.pgen.1008425.
52. Grkovic, S., Brown, M.H., and Skurray, R.A. (2002). Regulation of bacterial drug export systems. Microbiol Mol Biol Rev *66*, 671-701, table of contents. 10.1128/MMBR.66.4.671-701.2002.
53. Martinez, B., Bharati, B.K., Epshtein, V., and Nudler, E. (2022). Pervasive Transcription-coupled DNA repair in E. coli. Nature communications *13*, 1702. 10.1038/s41467-022-28871-y.
54. Wang, B., Pei, H., Lu, Z., Xu, Y., Han, S., Jia, Z., and Zheng, J. (2022). YihE is a novel binding partner of Rho and regulates Rho-dependent transcription termination in the Cpx stress response. iScience *25*, 105483. 10.1016/j.isci.2022.105483.

55. Roy, G., Antoine, R., Schwartz, A., Slupek, S., Rivera-Millot, A., Boudvillain, M., and Jacob-Dubuisson, F. (2022). Posttranscriptional Regulation by Copper with a New Upstream Open Reading Frame. mBio *13*, e0091222. 10.1128/mbio.00912-22.
56. Hafeezunnisa, M., and Sen, R. (2020). The Rho-Dependent Transcription Termination Is Involved in Broad-Spectrum Antibiotic Susceptibility in Escherichia coli. Front Microbiol *11*, 605305. 10.3389/fmicb.2020.605305.
57. Kriner, M.A., and Groisman, E.A. (2015). The Bacterial Transcription Termination Factor Rho Coordinates Mg(2+) Homeostasis with Translational Signals. J Mol Biol *427*, 3834-3849. 10.1016/j.jmb.2015.10.020.
58. Herrero Del Valle, A., Seip, B., Cervera-Marzal, I., Sacheau, G., Seefeldt, A.C., and Innis, C.A. (2020). Ornithine capture by a translating ribosome controls bacterial polyamine synthesis. Nat Microbiol *5*, 554-561. 10.1038/s41564-020-0669-1.
59. Gong, F., and Yanofsky, C. (2003). Rho's role in transcription attenuation in the tna operon of E. coli. Methods Enzymol *371*, 383-391.
60. Takemoto, N., Tanaka, Y., and Inui, M. (2015). Rho and RNase play a central role in FMN riboswitch regulation in Corynebacterium glutamicum. Nucleic Acids Res *43*, 520-529. 10.1093/nar/gku1281.
61. Jeon, H.J., Lee, Y., N, M.P.A., Wang, X., Chattoraj, D.K., and Lim, H.M. (2021). sRNA-mediated regulation of gal mRNA in E. coli: Involvement of transcript cleavage by RNase E together with Rho-dependent transcription termination. PLoS Genet *17*, e1009878. 10.1371/journal.pgen.1009878.
62. Sedlyarova, N., Shamovsky, I., Bharati, B.K., Epshtein, V., Chen, J., Gottesman, S., Schroeder, R., and Nudler, E. (2016). sRNA-Mediated Control of Transcription Termination in E. coli. Cell *167*, 111-121 e113. 10.1016/j.cell.2016.09.004.
63. Kriner, M.A., and Groisman, E.A. (2017). RNA secondary structures regulate three steps of Rho-dependent transcription termination within a bacterial mRNA leader. Nucleic Acids Res *45*, 631-642. 10.1093/nar/gkw889.
64. Repoila, F., and Gottesman, S. (2001). Signal transduction cascade for regulation of RpoS: temperature regulation of DsrA. J Bacteriol *183*, 4012-4023. 10.1128/JB.183.13.4012-4023.2001.
65. McCullen, C.A., Benhammou, J.N., Majdalani, N., and Gottesman, S. (2010). Mechanism of positive regulation by DsrA and RprA small noncoding RNAs: pairing increases translation and protects rpoS mRNA from degradation. J Bacteriol *192*, 5559-5571. 10.1128/JB.00464-10.
66. Sledjeski, D.D., Gupta, A., and Gottesman, S. (1996). The small RNA, DsrA, is essential for the low temperature expression of RpoS during exponential growth in Escherichia coli. EMBO J *15*, 3993-4000.
67. Simon, I., Delaleau, M., Schwartz, A., and Boudvillain, M. (2021). A Large Insertion Domain in the Rho Factor From a Low G + C, Gram-negative Bacterium is Critical for RNA Binding and Transcription Termination Activity. J Mol Biol *433*, 167060. 10.1016/j.jmb.2021.167060.
68. Chatterjee, S., Jiang, W., Emerson, S.D., and Inouye, M. (1993). The backbone structure of the major cold-shock protein CS7.4 of Escherichia coli in solution includes extensive beta-sheet structure. J Biochem *114*, 663-669. 10.1093/oxfordjournals.jbchem.a124234.
69. Figueroa-Bossi, N., Balbontin, R., and Bossi, L. (2023). Scarless DNA Recombineering. Cold Spring Harb Protoc *2023*, 638-650. 10.1101/pdb.prot107857.
70. Datsenko, K.A., and Wanner, B.L. (2000). One-step inactivation of chromosomal genes in Escherichia coli K-12 using PCR products. Proc Natl Acad Sci U S A *97*, 6640-6645. 10.1073/pnas.120163297.
71. Figueroa, N., Wills, N., and Bossi, L. (1991). Common sequence determinants of the response of a prokaryotic promoter to DNA bending and supercoiling. EMBO J *10*, 941-949. 10.1002/j.1460-2075.1991.tb08028.x.
72. Miller, J.H. (1992). A short course in bacterial genetics : a laboratory manual and handbook for Escherichia coli and related bacteria (Cold Spring Harbor Laboratory Press).

73. Schwartz, A., Rahmouni, A.R., and Boudvillain, M. (2003). The functional anatomy of an intrinsic transcription terminator. EMBO J *22*, 3385-3394. 10.1093/emboj/cdg310.
74. Diesh, C., Stevens, G.J., Xie, P., De Jesus Martinez, T., Hershberg, E.A., Leung, A., Guo, E., Dider, S., Zhang, J., Bridge, C., et al. (2023). JBrowse 2: a modular genome browser with views of synteny and structural variation. Genome Biol *24*, 74. 10.1186/s13059-023-02914-z.
75. Molodtsov, V., Wang, C., Firlar, E., Kaelber, J.T., and Ebright, R.H. (2023). Structural basis of Rho-dependent transcription termination. Nature. 10.1038/s41586-022-05658-1.
76. Hao, Z., Svetlov, V., and Nudler, E. (2021). Rho-dependent transcription termination: a revisionist view. Transcription *12*, 171-181. 10.1080/21541264.2021.1991773.

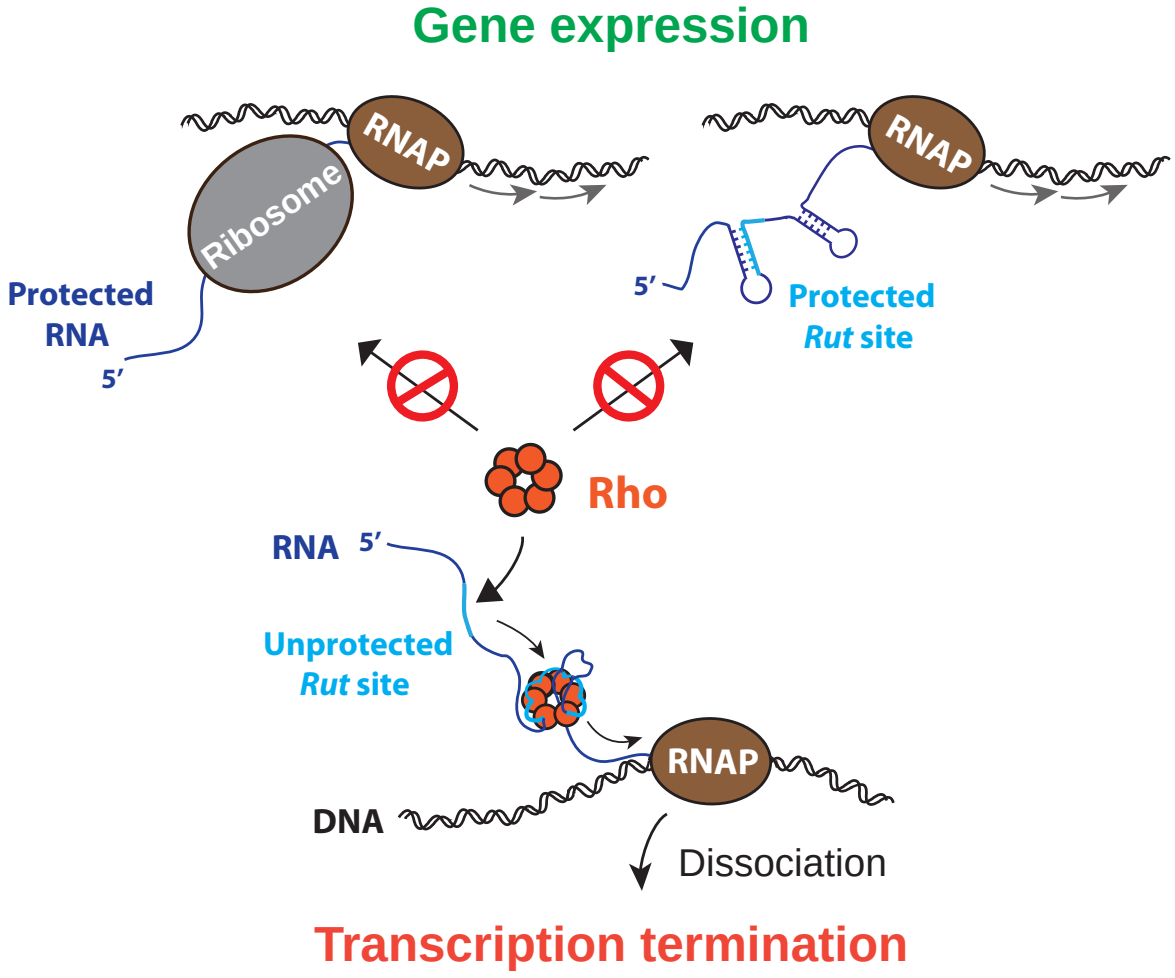

Figure 1: Rho-dependent termination. Rho binds to free *Rut* sites within nascent transcripts and then uses its ATP-dependent motor activity to catch up with RNA polymerase (RNAP) along the RNA chain and to trigger the dissociation of the transcription elongation complex (bottom) (Molodtsov et al., 2023). Rho action is prevented by the presence of translating ribosomes or by secondary structures in the nascent transcript that block Rut sites (top). In an alternative termination pathway, Rho binds RNAP early on during transcription and detects accessible *Rut* sites in the nascent transcript from this RNAP-bound position (Hao et al., 2021), which is not represented here for simplicity.

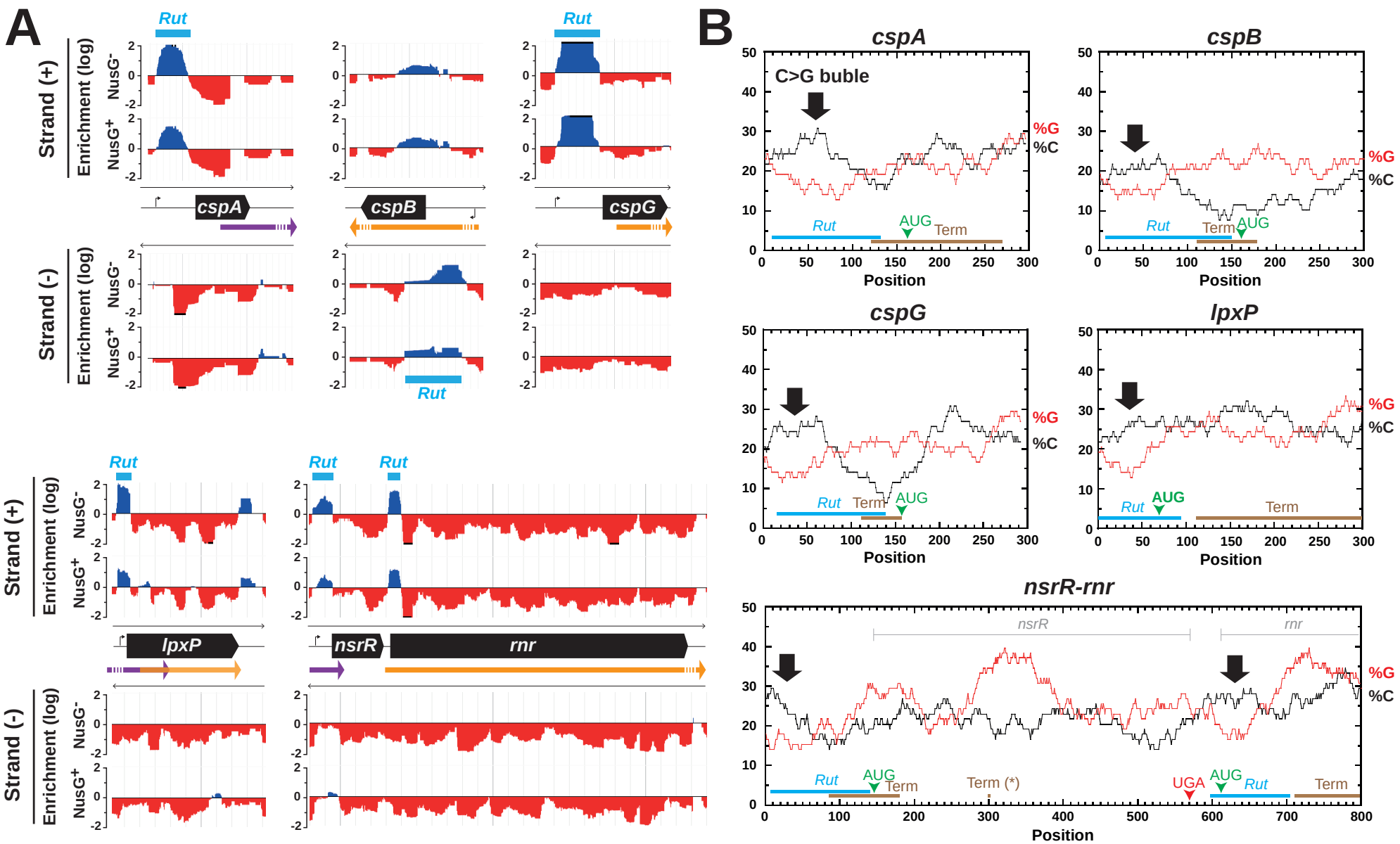

Figure 2: Putative *Rut* sites in the 5'-UTRs of *E. coli* genes involved in the CSR. **(A)** Fold enrichment (FE; $\log_{10}$ scale) profiles for Helicase-SELEX experiments performed with Rho in presence or absence of NusG were determined from published data (Delaleau et al., 2022). Cyan bars highlight the positions of the enrichment peaks (median $\log_{10}$FE ≥ 0.3) suggestive of *Rut* sites in the 5'UTRs. Regions where transcription is upregulated *in vivo* in presence of the Rho inhibitor Bicyclomycin, as determined by ChIP-chip (orange arrows; (Peters et al., 2009)) or microarrays and RNAseq (purple bars; (Peters et al., 2012)) are also shown. Note that different scales along the genome coordinates (x axis) are used for the various panels. **(B)** C>G bubbles (black arrows) overlap with the *Rut* peaks detected by Helicase-SELEX (cyan lines) and are present upstream from the *in vitro* transcription termination regions (brown lines), a feature characteristic of Rho-dependent terminators. Percentages of C and G residues were calculated using a sliding window of 78 nucleotides. Termination boundaries were estimated with the molecular size calibration/calculation function of ImageQuant software using *in vitro* transcription gel lanes.

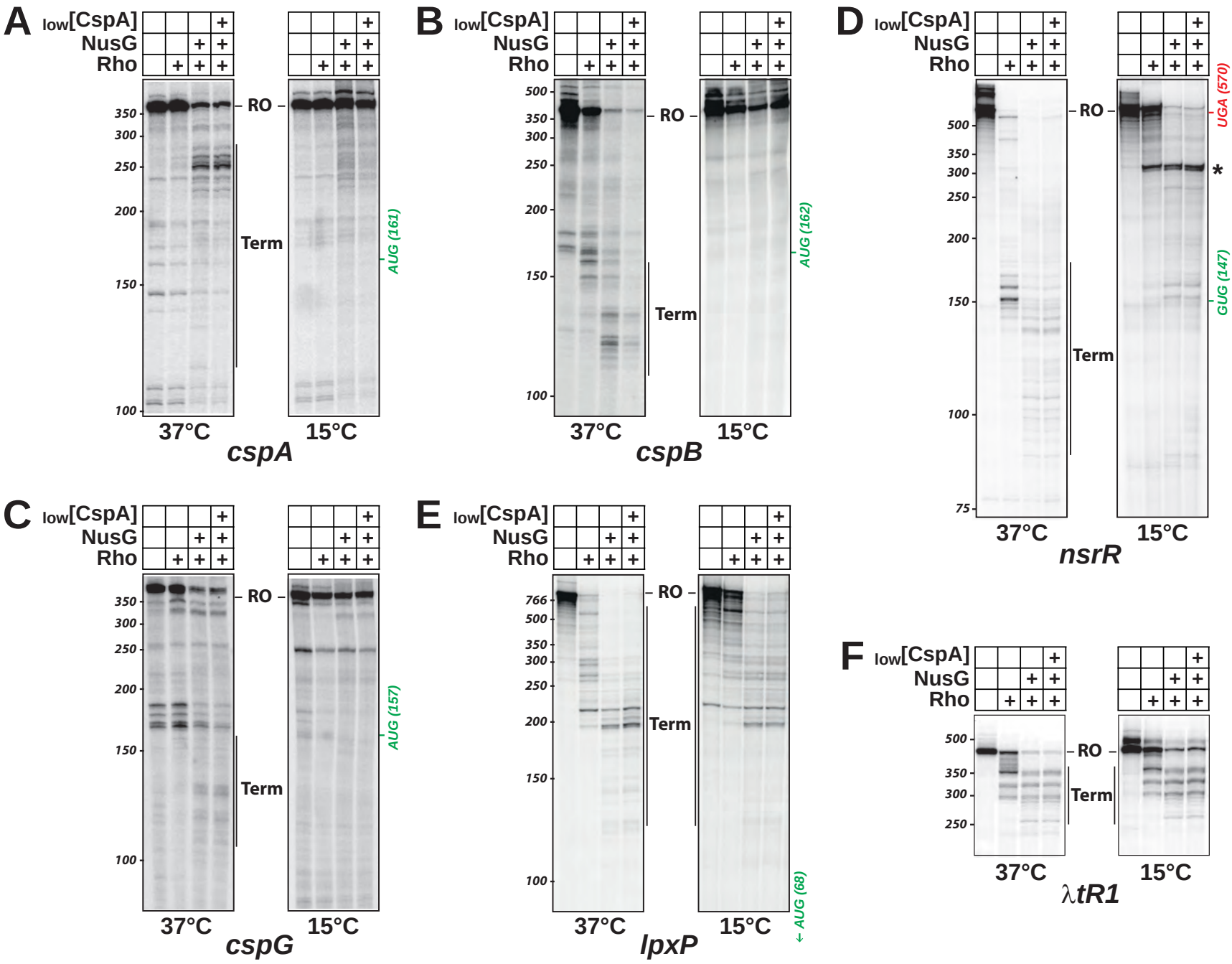

Figure 3: Cold shock genes contain Rho-dependent terminators in their 5'UTRs. Representative gel images show the *in vitro* transcription profiles obtained with DNA templates encoding the upstream sections of the E. coli *cspA*, *cspB*, *cspG*, *lpxP* and *nsrR* transcription units **(A-E)** or the λtR1 terminator **(F)**. Transcription reactions were performed at 15 or 37°C with or without Rho (20 nM), NusG (70 nM), or CspA (0.5 μM), as indicated. Bands corresponding to runoff (RO) and termination (Term) transcripts are indicated. Since transcripts are labeled by incorporation of α^{32}P-UTP during transcription, band intensities reflect both the amounts and sizes of the transcripts. A downstream nsrR termination site (*) is detected at 15°C (panel D).

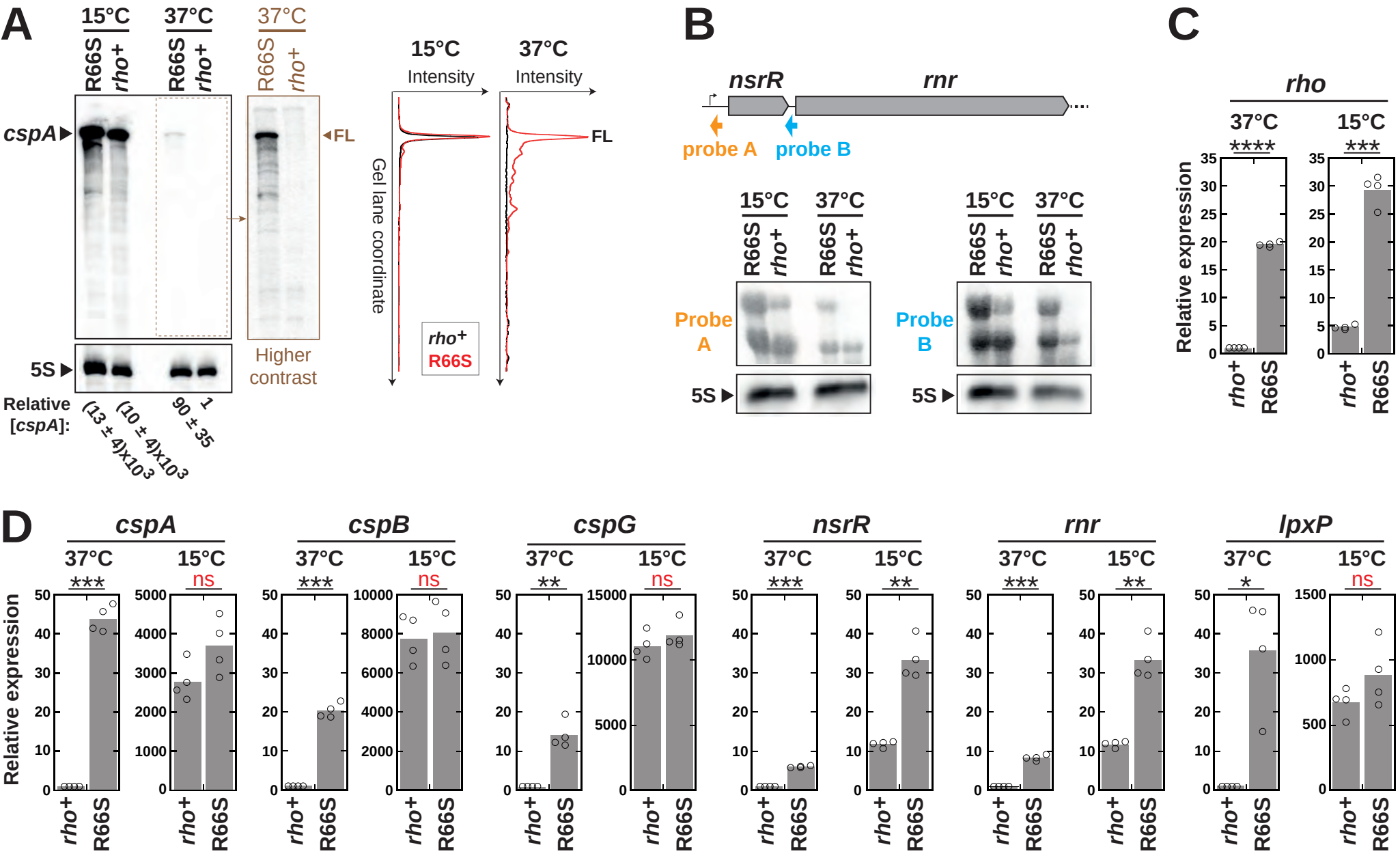

Figure 4: Transcription of cold shock genes is regulated by Rho *in vivo*. *E. coli* log phase cultures (A_{600} ~ 0.5) were incubated for 30 min at 15°C or 37°C before RNA extraction. **(A, B)** Northern blot analysis of the expression of *cspA* and *nsrR* in WT (*rho*$^{+}$) and *rho*^{R66S} (R66S) strains. Phosphorimager *cspA* counts were normalized to 5S RNA and the resulting values were divided by that obtained for WT at 37°C. The [*cspA*] values are (mean ± SD) values from three independent biological replicates. Pairwise comparisons of the normalized WT and R66S signals along gel lanes are provided on the right of the *cspA* membrane images (FL: full-length transcripts). Polycistronic *nsrR-rnr-yjfHI* transcripts are subjected to complex posttranscriptional processing (Cairrao and Arraiano, 2006; Cairrao et al., 2003) and were not quantified. **(C, D)** RT-qPCR confirms Rho-dependent regulation of cold shock genes. For each gene, signals are normalized to the condition *rho*$^{+}$, 37°C. Four biological replicates were analyzed by RT-qPCR, each time in triplicate (open circles represent the triplicate means). Statistical significance was determined by unpaired two-tailed Student's t-tests (ns, $p > 0.05$; *, $p < 0.05$; **, $p < 10^{-2}$; ***, $p < 10^{-3}$; ****, $p < 10^{-4}$).

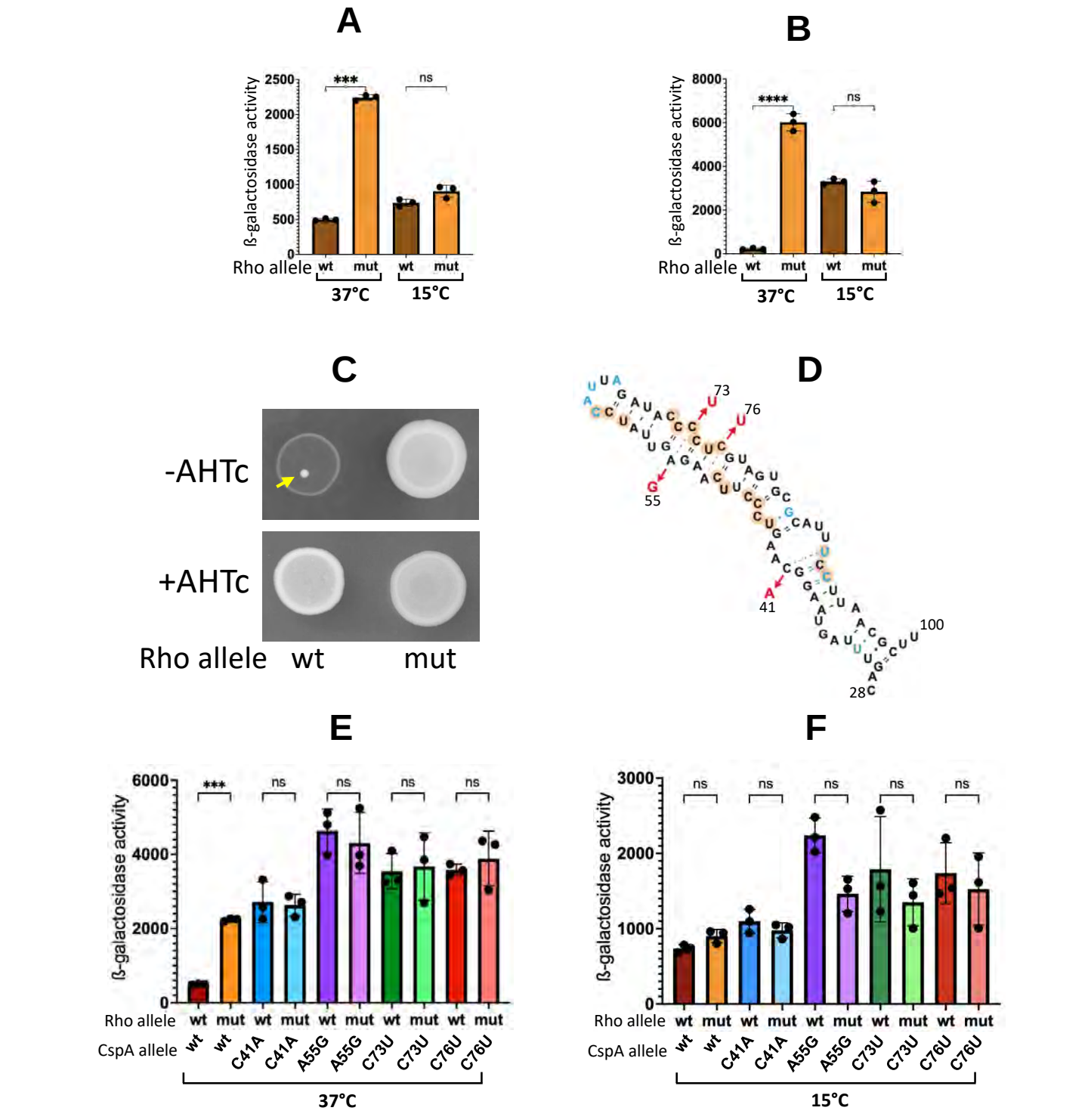

Figure 5. Mutations in the *cspA* leader RNA prevent Rho-dependent transcription termination in *Salmonella*. (**A, B**) Impact of Rho mutation Y80C on *cspA-lacZY* expression. Isogenic strains carrying the *cspA-lacZY* fusion under control of the P^{tet} promoter and either *rho*$^{+}$ or *rho*^{Y80C} were cultured in LB at 37°C until reaching mid-exponential phase (DO_{600} ≈ 0.4 - 0.5). At this point, expression of the *cspA-lacZY* fusion was induced by adding the P^{tet} inducer AHTc. The cultures were then divided, with one half transferred to 15°C and the other maintained at 37°C, and both were further incubated for (**A**) 30 and (**B**) 180 min. Cells were then processed for the determination of β-galactosidase activity. (**C**) Lac phenotype of strains carrying the P^{tet}-*cspA-lacZY* fusion in combination with either *rho*$^{+}$ (strain MA14635) or *rho*^{Y80C} (strain MA14636). Bacteria were cultured to stationary phase and 10 µl were spotted on minimal-lactose plates ±AHTc (37°C). The strain carrying *rho*^{Y80C} is Lac^{+} under non-inducing conditions (-AHTc) whereas the *rho*$^{+}$ strain is Lac^{-}. The yellow arrow highlights a Lac^{+} colony forming of the lawn of *rho*$^{+}$ cells. (**D**) Position of mutations suppressing the inhibitory effect of Rho on *cspA-lacZ* expression at 37°C . (**E, F**) Effect of the mutations in **D** on the expression of the *cspA-lacZ* fusion in the presence or absence of Rho Y80C at 37°C (**E**) and at 15°(**F**). Cells were cultured and treated as described in (**A, B**) with a time of incubation of 30 min after AHTc induction. Throughout this experiment, β-galactosidase activity was assayed with the method of Miller (Miller, 1992) on three independent replicates of the bacterial cultures, with each assay carried out in duplicate. Statistical significance was determined by one-way ANOVA with *Šidák's* multiple comparisons test (ns, $p > 0.05$; ***, $p \leq 10^{-3}$; ****, $p \leq 10^{-4}$).

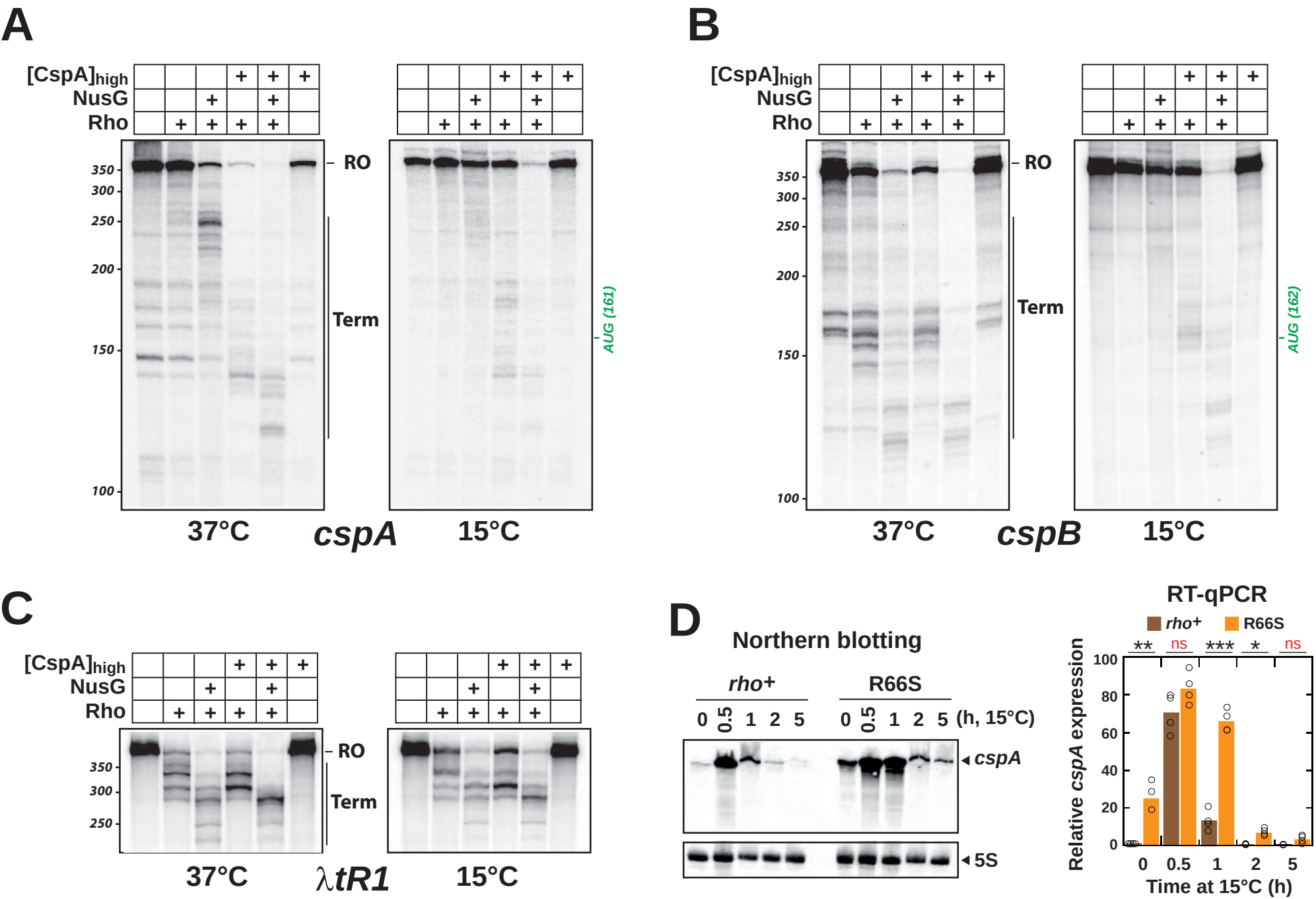

Figure 6: A high concentration of CspA stimulates Rho-dependent termination at *E. coli csp* terminators. Transcription experiments were performed with the *cspA* **(A)**, *cspB* **(B)** and control λtR1 **(C)** DNA templates as described in the legend to Figure 3, except that a 200-fold higher concentration of CspA was used (100 vs 0.5 µM). **(D)** Northern blot and RT-qPCR analyses of Rho-dependent attenuation of *cspA* as a function of the duration of the incubation at 15°C following cold shock. Four biological replicates were analyzed by RT-qPCR, each time in triplicate (open circles represent the triplicate means). Statistical significance was determined by unpaired two-tailed Student's t-tests (ns, $p > 0.05$; *, $p < 0.05$; **, $p < 10^{-2}$; ***, $p < 10^{-3}$).

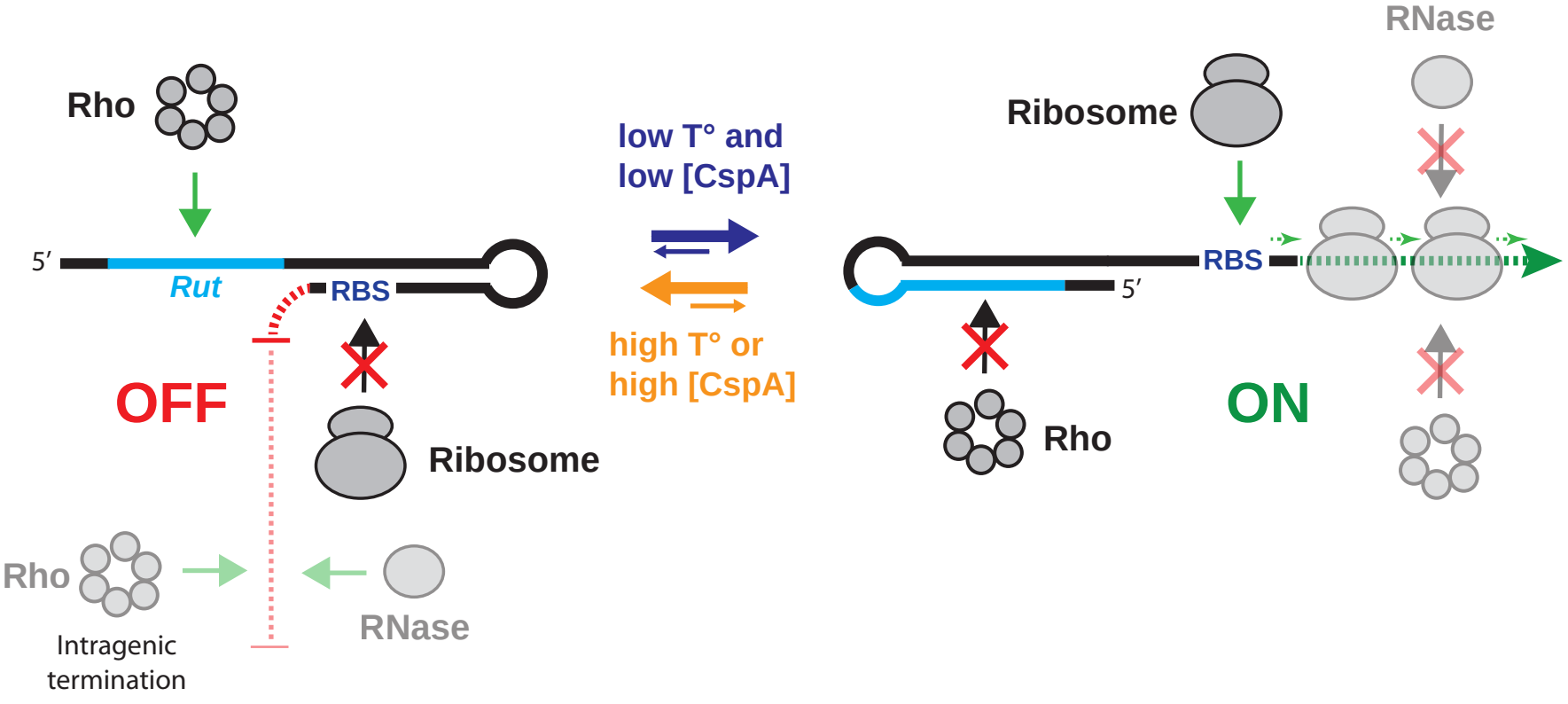

Figure 7: Model for regulation of *csp* genes. (**Left**) Rho-dependent attenuation of transcription in the 5'UTR inhibits *csp* expression at 37°C. Poor translatability of the transcripts that escape termination further contributes to *csp* down-regulation directly (Giuliodori et al., 2010; Yamanaka et al., 1999; Zhang et al., 2018) and, possibly indirectly, by facilitating intragenic transcription termination or RNA degradation or both (Fang et al., 1997). (**Right**) Restructuring of the 5'-leader upon the cold shock hides the *Rut* site and prevents premature transcription termination, at the same time enhancing the accessibility of the ribosome binding site. Protection of the CDS by translating ribosomes may contribute to stabilize the mRNA. During cold acclimation, the concentration of Csp proteins increases until it becomes sufficient to promote Csp binding to the mRNA. Csp binding drives the mRNA into a conformation that resembles the "37°C-conformation" (Zhang et al., 2018) and thereby restores attenuation.